UNIVERSITÀ DEGLI STUDI DI BERGAMO

Facoltà di Economia

Dottorato in Metodi Computazionali

per le Previsioni e Decisioni Economiche e Finanziarie

XXIV Ciclo

A STATISTICAL CHARACTERIZATION OF WIND GENERATION AND DEVELOPMENT OF A STOCHASTIC LP MODEL FOR THE SOLUTION OF THE UNIT COMMITMENT PROBLEM IN POWER SYSTEMS WITH HIGH RES PENETRATION

Relatore:

Chiar.ma Prof.ssa Maria Teresa Vespucci

Tesi di Dottorato

Dario SIFACE

Matricola n. 1008503

Contents

Chapter 1

Introduction

The present work describes the research activities I carried out in the last two years of my PhD course and it is divided in two main parts.

The first part, presented in chapters 2 to 7 under the title "*A Statistical Characterization of Wind Generation in Spain*", is focused on the research activity I carried out in 2010 at Instituto de Investigación Tecnologica of Universidad Pontificia Comillas in Madrid under the supervision of prof. Andres Ramos and his research team. This activity consisted on a statistical analysis of hourly wind generation and electric energy demand data from the Spanish power system with the intent to study the behavior of wind generation with respect to the energy demand in order to underline possible critical situations for power system operation.

The second part is described in chapters 8 to 11 and it deals with the development of a medium term zonal market simulator based on stochastic programming techniques for the solution of the hourly Unit Commitment problem in Power Systems with high levels of Renewable Energy Sources penetration. This activity has been carried out in 2011 at RSE SpA under the supervision of dott. Alberto Gelmini and has been financed by the Research Fund for the Italian Electrical System under the Contract Agreement

between RSE (formerly known as ERSE) and the Ministry of Economic Development - General Directorate for Nuclear Energy, Renewable Energy and Energy Efficiency stipulated on July 29, 2009 in compliance with the Decree of March 19, 2009.

Chapter 2

A Statistical Characterization of Wind Generation in Spain

2.1 Introduction

In the last two decades the interest in renewable generation of electricity has largely increased in the world, in order to lower the dependence from fossil fuels which is imported by many nations, and mainly the European ones.

The reasons of this are both environmental (mitigation of the impact of emissions on the climate change) and economical (continuous increase of fuel price). In the Kyoto protocol international agreement these two main reasons come to coincide, since the unfulfillment of environmental aims by a state results in economic penalties.

Among the various possible renewable sources, one of the most developed is wind (**WG**), since it is available all over the world, even if with great local differences, and its operating costs are almost zero.

Anyway, WG has some great disadvantages: firstly, it is partially out of the human control; secondly, it is greatly intermittent, with strong vari-

ations even on hourly basis; furthermore, forecasting error on wind speed could lead to huge forecasting error in energy production due to the strong nonlinear behavior of wind turbine power curves (see [1]).

All these considerations lead to develop a large number of investigations either on the economical impact of the introduction of WG in existing national electrical networks (examples are [2], [3], [4]) and its various aspects, either on its effects on interconnections of networks of different countries (examples are [5], [6], [7]).

Another important issue worth of being investigated is the behavior of WG with respect to the Electricity Demand (**Dem**), in order to evaluate the potential of WG in an electric system.

This topic is not trivial since, as we have already underlined, the intermittency of WG is strong and cannot be controlled. This is the reason why the topic is investigated by a number of papers; two of them, both referring to UK electricity market, are particularly interesting: [8] and [9].

The first paper, [8], sets out to assess how consistent wind power is likely to be in the UK, and the consequences of any volatility on the control and utilization of individual generation plant on the grid. This is achieved by means of modeling the dynamical behavior of 25 GW of wind on the UK grid system.

This analysis is limited to the month of January which reveals to be, for the UK system, both the month of peak demand and of highest wind output; data from 12 consecutive years are considered.

The approach is not statistical, since, according to the authors, the study focuses on the worst possible conditions (i.e. the most challenging ones) in

order to examine how individual generators and operators would have to react to these new operational conditions.

The model considered consists on 8 sites of generation situated in different places all over Great Britain island, with a total installed capacity of 25 GW. Generation data are extrapolated from wind speed data at ground.

Among the results obtained in this study, the most interesting are:

- a high degree of volatility is present in the entire grid, even if the different production sites are distant from one another;
- the high volatility degree introduced into the grid along with wind generation bring with itself a lesser reliability degree of the grid itself, with the consequent necessity of building more thermal plants; this means an increase in costs, both economical and environmental;
- low wind periods may correspond to high demand periods.

On the other side, [9] performs an analysis of the characteristics of the wind power resource of the UK in order to examine the relationship between WG and electricity demand, both calculated on an hourly basis.

What is put in evidence by the author is that even if correlation values between WG and Dem are quite low, on average, in hours of Dem peaks a CF[1] higher than the average of the whole set of hours in a year can be found. Then, considering extreme Dem values, that is peak and off-peak hours, again it is confirmed that the probability of finding high WG values during peak hours is higher than the average and that wind power output during hours of low wind electricity demand is less than half that of the long-term annual average output.

[1]Capacity Factor is defined as the ratio of electricity produced over the maximal production of WG.

Informations coming out from studies such as [8] and [9] are thus very useful. This is the reason why in this paper we perform a similar study for the Spanish system. With the following main difference. Both in [8] and [9], in fact, WG output is calculated starting from wind speed data and wind turbine power curves. This procedure allows to increase greatly the amount of data that could be studied, since historical wind speed data can easily be found in weather offices data bases even for years in which no real wind farms were existing. The disadvantage is that power output must be modeled by means of hypotheses that cannot be totally realistic, such as:

- all production sites use the same type of wind generator; and
- use of interpolated wind speeds at the wind farm height, since wind speed data refer to ground speed.

Since we have access to four complete years of WG historical data, enough to perform our statistical analyses, we were able to avoid these disadvantages.

In chapter 3 the sources of our data are presented, as well as the mathematical and statistical devices we used to study them; in chapter 4 daily behavior of Dem and WG is showed; in chapter 5 correlation analysis of Dem and WG data series is performed in order to individuate and classify critical periods during the year. In chapter 6 we will perform a study of the statistical characterization of WG by means of cluster analysis.

Conclusions of studies performed in chapters 5 and 6 are presented in chapter 7.

Finally, two appendices are added: Appendix A explains how Theory of Cluster Analysis can be applied to our study; Appendix B shows the development of a technique to perform statistical tests with null hypothesis over intervals of values.

Chapter 3

Data Sources

We have considered hourly data for Dem and WG in Spain for every day in the four years from mid 2006 to mid 2010, coming from [10].

Non-working days' Dem values are typically a 20% lower than the one of working days; on the contrary WG is not affected by this "*non-working day effect*". This is why we conducted the analysis concerning both Dem and WG only for working days and so the number of days is reduced accordingly.

3.0.1 Data Discounting and Data Normalization

Both total Demand and WG installed capacity were varying during the years under analysis. In particular, installed capacity for WG has increased highly from year to year[1]. Thus, in order to confront data coming from different years, we had to discount or normalize them.

For what concerns discounting, we assumed a linear rate of change during any year; that is: given the installed capacity at the end of previous year b and the variation rate t (positive or negative), then the installed power at the end of the year under analysis is $e = b(1 + t)$. For a general time span (which usually is a day or a month), given the number of time spans of this

[1]Variation rates for Dem and WG came from [11].

kind in this year n ($n = 12$ if we are dealing with months or $n = 365$ if we are dealing with days in a normal year), then the discounted production value in time span d, $\overline{WG}_d$, comes out from

$$\overline{WG}_d = \frac{WG_d}{1 + t\frac{d}{n}}, \tag{3.1}$$

where WG_d is the real production value in time span d. The same approach can be used for Dem, leading to equation

$$\overline{Dem}_d = \frac{Dem_d}{1 + t\frac{d}{n}}, \tag{3.2}$$

For what concerns WG normalization, it is performed using the installed capacity on a monthly basis a_m, which can be calculated, given the installed capacity a_0 at the end of the previous year and the increasing rate t for year under analysis, by means of the following formula

$$a_m = a_0(1 + t\frac{m}{12}). \tag{3.3}$$

Chapter 4

Demand versus Wind Generation

In this section we will describe the daily characterization of Dem and WG

4.1 Demand Curve

If we plot the value of Dem with respect to the hours of one day, as in fig. 4.1, we can obtain a very typical pattern which shows practically no or very little variations between consecutive working days[1], for what concerns both shape and values.

We can now look at this particular pattern to better underline its peculiarities.

Starting from the 1^{st} hour in the day, we can see a regular decrease in demand which ends in the 6^{th}, when we can find the first, and lowest, minimum of daily demand.

Then, for the next 6 hours, an increase in demand takes place, so that in

[1]Differences, even of wide entity, actually occur between working and non-working days

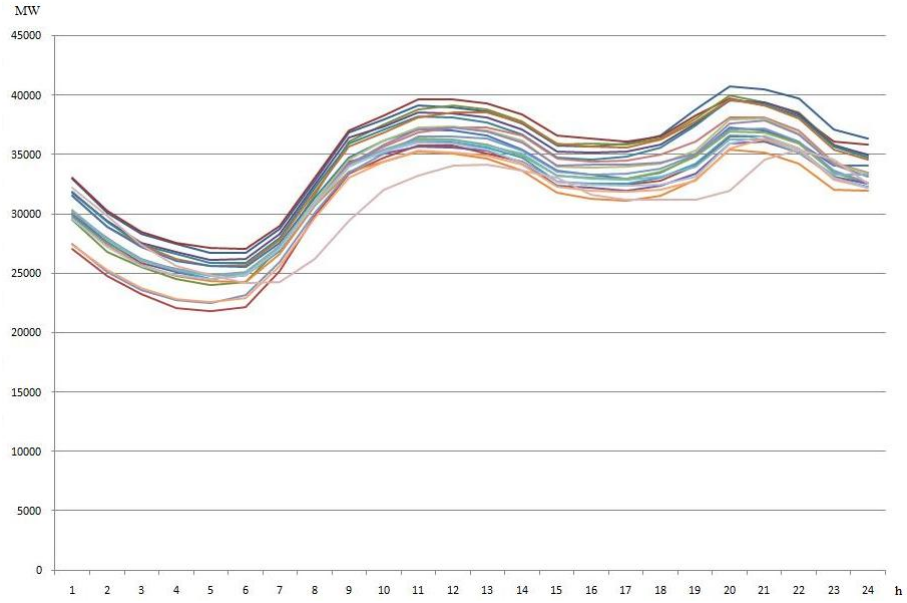

Figure 4.1: Hourly profile of Dem during different working days in February 2007

the 12^{th} hour we encounter the first maximum.

From hour number 12 to hour number 16 we encounter a light decrease followed by a similarly light increase in demand, until hour number 20, so that we have a second, local, minimum in hour 4 and a second maximum in hour 20; usually, this is the global maximum of the day, but the difference between this peak and the one in hour 12 is very small.

Finally the demand decreases continuously until hour 24.

4.2 Wind Generation Curve

As we have discussed in section 2.1, very strong differences in WG can occur, even between consecutive days. As a consequence, we cannot show a typical pattern as we did for Dem in section 4.1, as it is shown in fig. 4.2. Here it re-

sults evident how both shape and values are very different even for close days.

Then we have to perform a statistical study trying to find out groups

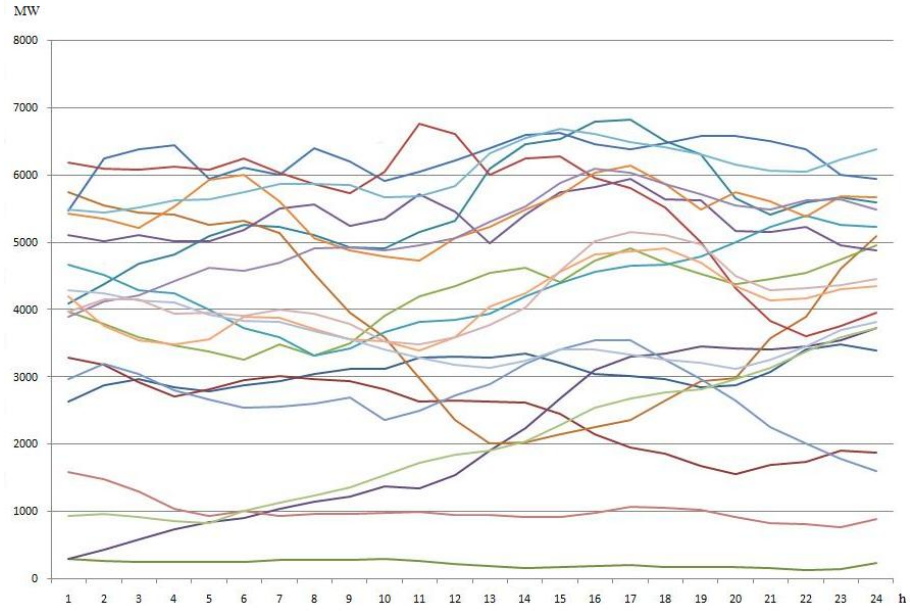

Figure 4.2: Hourly profile of WG during different working days in February 2007

of days with a similar behavior w.r.t. either the level of production or the shape of the production.

The way we can perform this statistical analysis is by building *clusters* of days with respect to WG, both w.r.t. the shape of the curve and the level of production. This will be performed in chapter 6.

4.3 Demand versus Wind Generation Curve

In previous sections we have presented analysis over Dem or WG alone. But often, the better way to perform this study is to take into account both of

them. In this way, in fact, is possible to obtain very interesting and useful informations, as we are going to show in the following sections.

4.3.1 Correlation Between Demand and Wind Generation

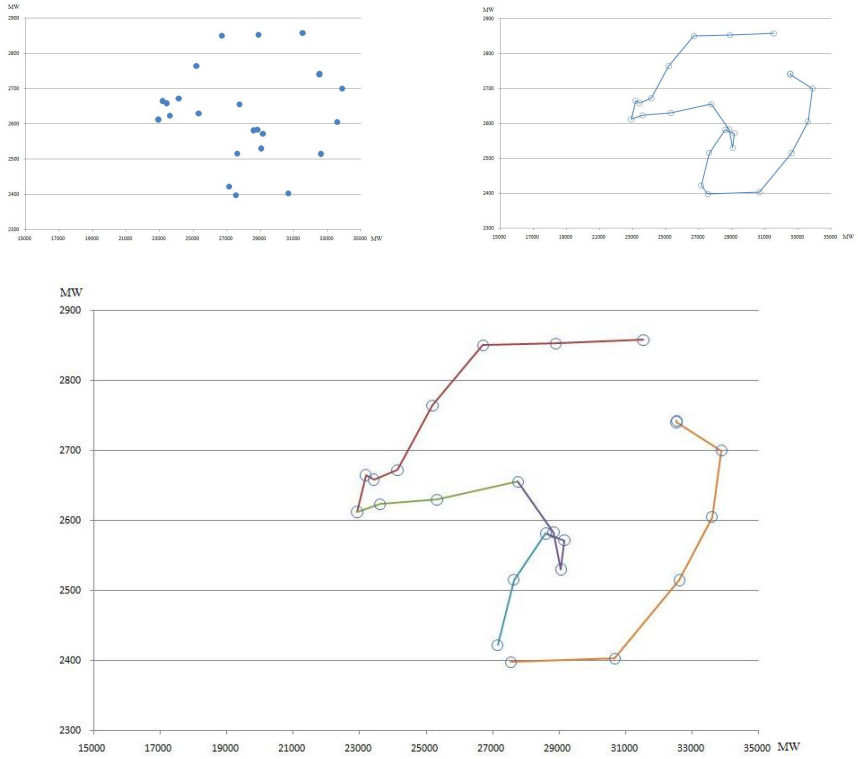

Figure 4.3: Dem (x axis) vs WG (y axis) plot for one day in July. We can isolate groups of consecutive hours forming nearly linear "branches".

We can plot WG versus Dem for all the 24 hours in a single day. What will come out is generally a cloud of 24 points with apparently no regularity (see fig. 4.3-a). But if we build the same plot taking into account the existence of subsequent hours, as in fig. 4.3-b, some interesting details become evident.

The resulting curve's shape may vary a lot from one day to another,

since it contains information coming both from Dem, which is very regular, and WG, which is very irregular. Anyway, in any case we can isolate some curve subsets which could also be called ***branches*** which are likely to be linear, as clearly can be seen in fig. 4.3-c. Each one of these branches indicates groups of subsequent hours during which Dem and WG show a strong correlation, either negative or positive.

4.3.2 Classification of Days by Means of Dem versus WG Curve

The existence of these branches can also be helpful in building clusters of days with a similar behavior. In fact, even if any single day has its particular curve shape, there exist groups of days with similar curve shape. This topic is deeply discussed in Appendix A and Chapter 6.

Here we will only show the example of July, with a sample consisting of around 80 days for any of the 24 hours of the day.

These days were divided into 20 clusters by means of Cluster Analysis (cfr. Appendix A). In figures 4.4 4 of these clusters are shown.

We can see how the shape of the Dem versus WG curves in the same cluster are similar, even if the levels of Dem and WG can vary.

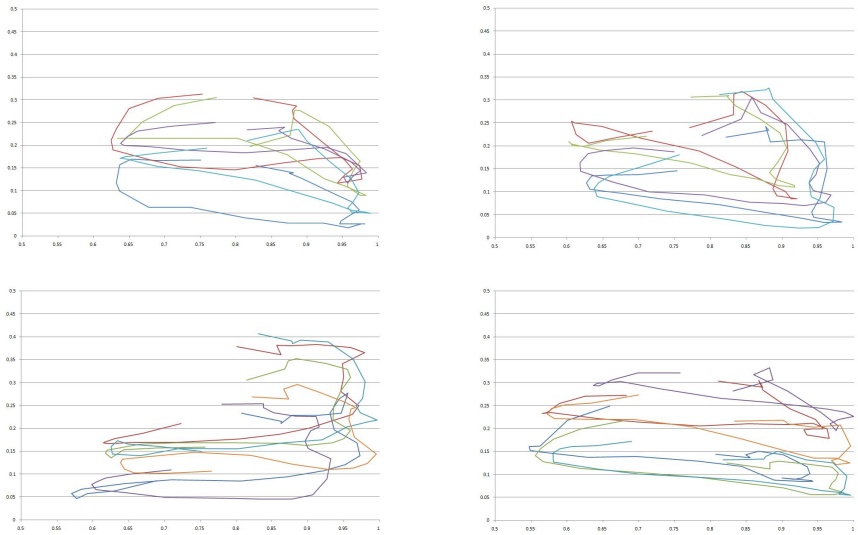

Figure 4.4: Dem vs WG curve in July - cluster examples

Chapter 5

Correlation Between Demand and Wind Generation

In this section we will show the results of the statistical analysis about the presence of correlation between Demand and Wind Generation data series.

We dealt with hourly data for Demand and Wind Generation. This allowed us to perform various different kinds of analyses; for example:

1. study what happens for a particular hour of the day in a particular month (e.g. 6.00 a.m. in January) or season;

2. study what happens during a particular day (e.g. November 6^{th} from 1.00 a.m. to 12.00 a.m.) or week.

By a logical point of view, the first approach should allow to verify the existence of a tendency typical of a single hour. This means that we are trying to verify if at the same hour every day Dem and WG behave in the same way w.r.t. each other. In order to perform this we considered only the values of Dem and WG for the chosen hour, for each day of the time span under analysis.

The second approach, on the other hand, should allow to verify the exis-

tence of a positive or negative tendency during the whole day. That is, we consider all the 24 hours values for Dem and WG for the chosen date.

5.1 Methodology

A theoretic definition of ***statistical correlation***, usually indicated by the mathematical symbol ρ, can be found in [12].

Two series can have a ***positive*** or ***negative*** correlation or can have ***no*** correlation. In case of two ***positively correlated series*** high values of the first series correspond to high values of the second one and low values of the first series correspond to low values of the second one.

Dealing with Dem and WG, if positive correlation would exist this would imply two important things: firstly that during Dem peaks we would have WG peaks, which could indicate that WG can help in sustaining Dem peaks; at the same time, that low values of WG would correspond to low values of Dem, which could indicate that there is low risk of energy spillage.

On the contrary, if two series show ***negative correlation*** high values of one series correspond low to values of the second. For what concerns Dem and WG, if this would be the case, this would mean that during Demand peaks, WG would be very low and could not help in sustaining it; on the contrary, in correspondence of minimum Demand we would encounter peaks of WG, with the risk of energy spillage.

In any case, presence of correlation, both negative or positive, between Dem and WG could be very helpful in decision-taking. But if ***no correlation*** exists, this would mean that both days in which Dem and WG have similar behavior and days in which they have opposite behavior may occur with similar probability resulting in no useful information for decision-taking

and, consequently, more conservative policies to be used.

In order to determine the correlation, statistical tests have to be performed and thus sentences like "*no correlation exists*" have no meaning: only can be affirmed that "*a significant correlation does/does not exist*" with a given probability α which is called "***significance level***".

Since we would like to be able to indicate values of correlation coefficient as non significant even if "*sufficiently close*" to 0, we developed a procedure for performing tests over the sample correlation r with null hypothesis of the form:

$$H_0 = \rho \in [\rho_1, \rho_2], \tag{5.1}$$

in which the ρ_i's can have whatever value in $[-1, 1]$. The mathematical development of this procedure, starting from the general theory found in [12], is explained in appendix B.

We have to remark that performing a statistical test with a level of significance α over a null hypothesis H_0 consists on verifying by statistical means if H_0 is false. In fact, as we can read in [12] and [13], if the test rejects H_0, we can be sure by a percentage equal to α that it is false, but if the test does not reject H_0 nothing can be said about it.

Once we have developed the above procedure and with the meaning of statistical tests in mind, we were able to perform the two kind of tests we needed: test if ρ is significantly close to 0 and, if not, if it's positive or negative.

We consider significantly close to 0 values of ρ belonging to the interval $(-0.1, 0.1)$. Then, the two tests performed has the following two null

hypothesis:

$$\begin{aligned} H_{0A_{out}} &:= \rho \notin (-0.1, 0.1) \\ H_{0A_{in}} &:= \rho \in (-0.1, 0.1) \end{aligned} \tag{5.2}$$

$$\begin{aligned} H_{0B_-} &:= \rho < 0 \\ H_{0B_+} &:= \rho > 0 \end{aligned} \tag{5.3}$$

We can divide the elements of our sample into 5 groups according to these definitions:

1. contains all the items for which were rejected $H_{0A_{in}}$ and H_{0B_+}; this means $\rho < -0.1$;

2. contains all the days for which was rejected only H_{0B_+}; this means that ρ is non-positive;

3. contains all the days with no significant correlation, that is for which was rejected $H_{0A_{out}}$;

4. contains all the days for which only H_{0B_-} was rejected; this means that ρ is non-negative;

5. contains all the days for which were rejected both $H_{0A_{in}}$ and H_{0B_-}; this means $\rho > 0.1$;

We developed an algorithm capable in choosing the correct null hypothesis depending on the value of the sample correlation r. The level of significance is always set to 95%.

5.2 Results

Here we present the results of the analysis performed.

5.2.1 Daily Analysis

First, we will show in figure 5.1 the results of the analysis of correlation between Dem and WG for all the 24 hours of a fixed day.

In figure 5.1-b the meaning of the colors is explained, as well as the

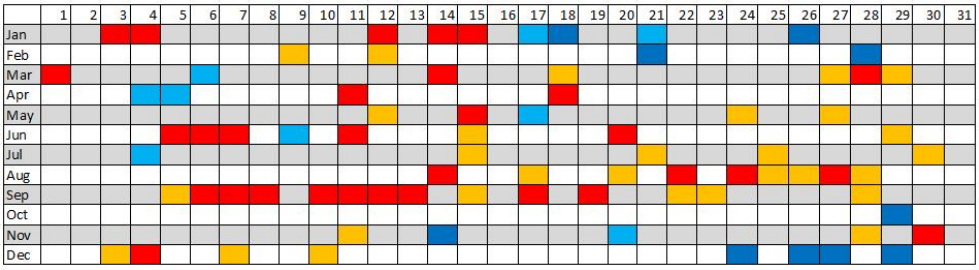

		H_{0Ain}	H_{0Aout}	H_{0B+}	H_{0B-}	#
	ρ < -0.1	R		R		31
	ρ < 0			R		29
	-0.1 < ρ < 0.1		R			0
	ρ > 0				R	9
	ρ > 0.1	R			R	10

Figure 5.1: Working days analysis: results (a) and colors explication (b)

number of days belonging to each group defined in section 5.1. Only 79 days in a whole year (i.e. about 21%) could be classified with a signifcance level of 95%.

We have to underline that the standard deviation of the distribution upon which the correlation test is based depends inversely on the number of elements belonging to the sample. Then, the more the hours we consider, the smaller the confidence interval of the test. Now we have samples consisting in 24 hours a day for each year we are considering. Thus, if we were able to consider more days or more years, we should be able to classify a larger amount of time.

Among the 79 classified days, no one showed no significant correlation and 60 show a negative tendency in correlation between Dem and WG. Fur-

thermore, the majority (34) of these days can be found between July and September (i.e. in summer) while only 2 of the 19 days showing positive tendency appear in this season.

5.2.2 Weekly Analysis

In figure 5.2 we present graphically the results of the same analysis above performed over a whole week. That is, we considered all the hours belonging to all the working days of any of the 53 weeks that form a year. We indicated any week with a number and indicated the month to which it belongs to, to better understand the effects of seasonality.

As above, in figure 5.2-b the meaning of the colors is explained, as well

Jan	1	2	3	4	5
Feb	6	7	8	9	
Mar	10	11	12	13	14
Apr	15	16	17	18	
May	19	20	21	22	
Jun	23	24	25	26	
Jul	27	28	29	30	31
Ago	32	33	34	35	
Sep	36	37	38	39	
Oct	40	41	42	43	44
Nov	45	46	47	48	
Dec	49	50	51	52	53

		H_{0Ain}	H_{0Aout}	H_{0B+}	H_{0B-}	#
	$\rho < -0.1$	R		R		5
	$\rho < 0$			R		14
	$-0.1 < \rho < 0.1$		R			4
	$\rho > 0$				R	8
	$\rho > 0.1$	R			R	0

Figure 5.2: Weekly analysis: results (a) and colors explication (b)

as the number of weeks belonging to each group. Here about the 59% (31 over 53) of the weeks can be classified with a significance level of 95%.

As we were expecting, having considered larger samples (a working week contains 5 days) than in section 5.2.1 allowed us to perform the test with higher precision and classify a larger amount of time (we passed from 21% to 59% of the year).

Of the 31 weeks classified, the majority (19) show a negative tendency. Furthermore, all the weeks between the end of June and the end of September (i.e. Summer), with the only exception of the last week of August, present a negative tendency. These two results appear to be confirmations of what we observed in section 5.2.1.

Other seasons do not show a tendency as clear as the one in summer.

5.2.3 Monthly Analysis

Here below, in figure 5.3 we will show the results of the analysis performed for any single month fixing an hour. For each month, any hour can be classified into the same 5 groups as done above (section 5.2.1) for days.

Only for 4 months a clear classification of hours could be done: June,

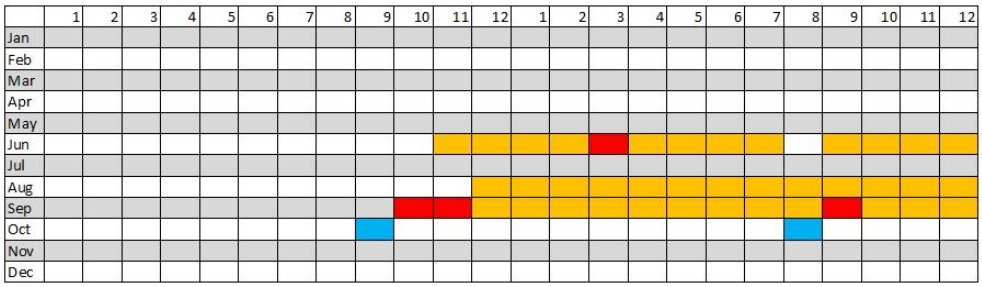

Figure 5.3: Monthly analysis results; red: negative correlation; orange: non-positive correlation; green: no correlation; light blue: non-negative correlation; dark blue: positive correlation

August and September, which are, again as in the previous analyses (sections 5.2.1 and 5.2.2), summer months, and October.

But while in summer months an uninterrupted negative tendency in cor-

relation appears in the second half of the day, in October a light positive tendency appears only at 9.00 a.m. and at 8.00 p.m.

5.2.4 Seasonal Analysis

Finally, in figure 5.4 we are going to show the results of the analysis performed for a fixed hour in a whole season. Again, for each season the 5 classification groups are the same as above.

Only for spring and summer a classification of hours can be done; in

Figure 5.4: Seasonal analysis results: red: negative correlation; orange: non-positive correlation; green: no correlation; light blue: non-negative correlation; dark blue: positive correlation

particular, for summer the whole day shows a negative tendency in correlation, that becomes stronger during the afternoon and evening hours. This appears as a confirmation of what observed in previous analysis (section 5.2.3), where the only months for which the classification could be done were June, August and September, but also of what observed in sections 5.2.1 and 5.2.2.

The increase in the number of hours that could be classified can be explained by the increase of the number of hours in each sample, as in section 5.2.2, since a season contains about 4 times more hours than a single month.

Chapter 6

Statistical Characterization of Wind Generation

The analysis of statistical correlation between Dem and WG performed in Chapter 5 revealed that in Spain during summer exists a negative tendency in correlation between Dem and WG, continuously spread during the whole day. The most negative effects this reciprocal behavior could result in are:

- the decrease in WG plus the increase in Dem implies that other generation devices must follow an apparently steeper upwards ramp, ΔDem, as drawn schematically in figure 6.1;
- a surplus of WG may happen in off-peak hours.

On the other side, for all the other periods of the year such an evident relationship between the two series cannot be found. This does not mean that the situation is more favorable in spring or winter than in summer, but only that the situation is less defined, not clearly characterized.

From the point of view of unit commitment, this could even be considered a worst condition, since knowing that the negative effects introduced above are likely to happen allows to commit the unit in advance. On the contrary, if a decrease of WG during Dem upwards ramp have a similar chance to

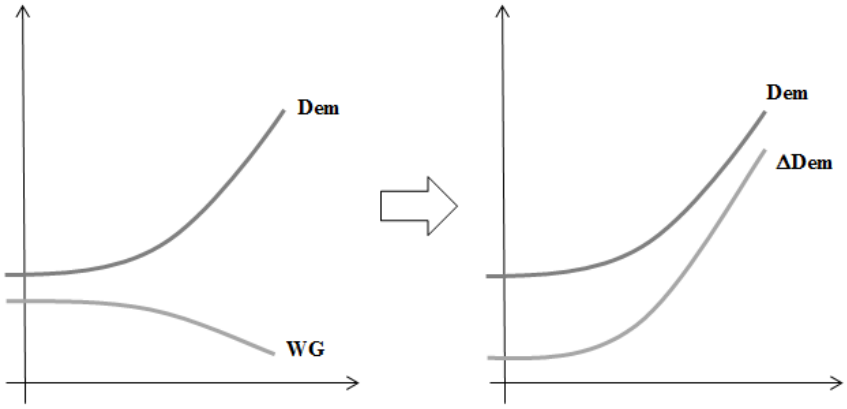

Figure 6.1: Increase of Dem upward ramp due to WG decrease

happen than an increase, what in the first case is a solution to the problem, in the second would be the problem.

We can now perform a deep analysis applying what was showed in Chapter 4, that is how to study the reciprocal behavior of Dem and WG in a day by means of finding groups of consecutive hours with an evident correlation between the two series.

In the same Chapter, we have analyzed and described the daily Dem pattern (see fig. 6.2) and in particular we can find three important characteristics:

- very little variations among working days of the same month
- a large increase between hour 6 and hour 12
- the daily minimum in the 6^{th} hour.

Under the considerations discussed above, these two characteristics of Dem daily profile become the two following critical issues:

- the main element of difference from day to day is WG

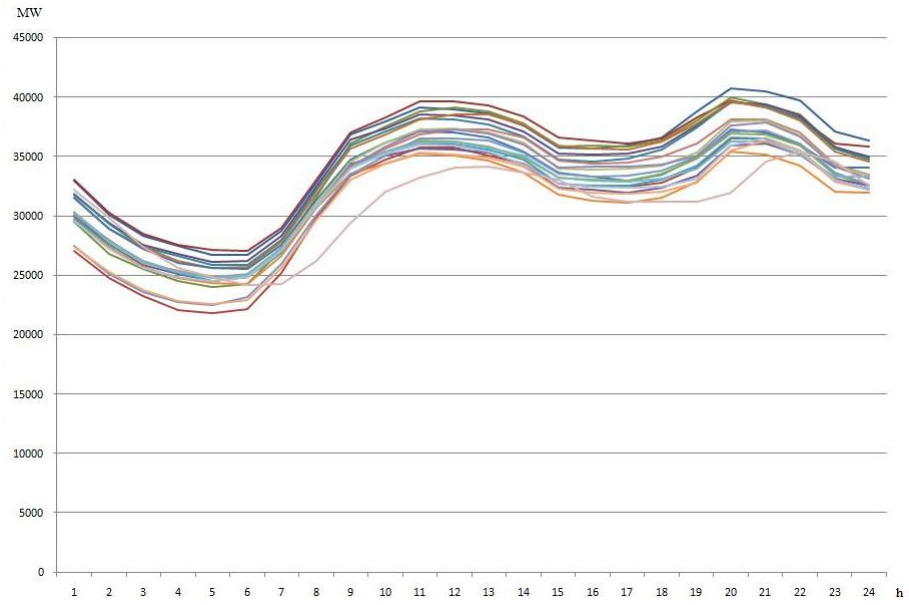

Figure 6.2: Hourly profile of Dem during different working days in February 2007

- the difference of generation between hour 6 and hour 12
- the generation in the 6^{th} hour.

thus any day in a month could be characterized only by means of a study over WG.

This characterization can also be used to individuate a limited number of "*representative days*", which should be more easily to handle than the hundreds of days we are now dealing with. To perform this task, we need the aid of *Clustering Analysis*, as described in appendix A.

In short, the operation named "***clustering***", consists of grouping similar items together and building for any new group a representative item. Is fundamental to define exactly what "*similar*" does mean and what peculiar characteristics the "*representative item*" must have.

For what concerns the present topics, each cluster contains all those days who minimize the "*euclidean distance*" between each day's ΔWG or WG values and the corresponding values of each cluster's representative day. This representative day is called "***centroid***" and it's ΔWG and WG values are calculated as the mean values of the cluster.

The greater the number of clusters, the better the approximation given by the centroid, but on the counterpart, the greater the number of clusters, the lower the advantage we gain in dealing with centroids instead of real days. Thus, a trade-off decision has to be taken to decide the correct number of cluster to use. This trade-off analysis led us to create 10 groups of days in each of the analysis performed.

6.1 Case of Study

We considered hourly data for WG in Spain for every day[1] from the four years of our sample.

As a case example we have focused only on two months:

- February: is the only winter[2] month without vacation days other than weekend days; furthermore, is characterized by high demand and revealed to be one of the most windy months of the year;

- July: is a Summer month[3] characterized by high Demand due to use of air conditioning systems but, at the same time, one of the less windy

[1] WG does not depend on the type of days to be working or non-working

[2] According to Chapter 5, Winter is a season with no certain characterization by means of statistical correlation between Dem and WG.

[3] According to Chapter 5, Summer is the only season in which we found a negative correlation between Dem and WG in the central hours of the day.

months of the year; is preferable to August since Spanish people use to go for vacation mainly in August.

6.1.1 Cluster Analysis

First of all, the representative days for each month, built accordingly to the theoretical considerations in appendix A, are shown. Subsequently it will be shown how the introduction of clusters reflects the real data in representing the statistical behavior of the real sample.

Values are normalized by means of monthly installed power, according to section 3.0.1.

February In figures 6.3 and 6.4 the 10 representative days are presented, each with it's percentage[4] value, for WG production in hour 6 and for difference in WG production between the 6^{th} and the 12^{th} hour respectively.

In figure 6.5 the historical cumulative distribution function for normalized WG production in hour 6 in February (blue line) is plotted with the one obtained from the distribution of representing days (red line); also representative days are indicated (yellow dots). The mean quadratic error between the two curves is 3.3%, then we can say that the accuracy of the representative days is good.

In figure 6.6 the historical cumulative density function for normalized ΔWG production between 6^{th} and 12^{th} hours in February (blue line) is plotted with the one coming out from the distribution of representing days (red line); also representing days are indicated (yellow dots). Since the mean quadratic error between the two curves value is 2.5%, it can be said again that the match between the two curves is good.

[4]Calculated as the relative frequency of occurrence

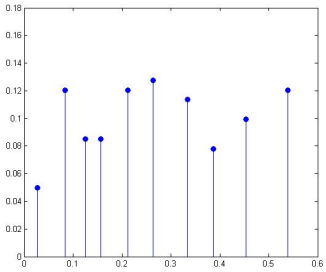

Figure 6.3: Representative days for WG in hour 6 in February, with their correspondent frequency percentage (y axis)

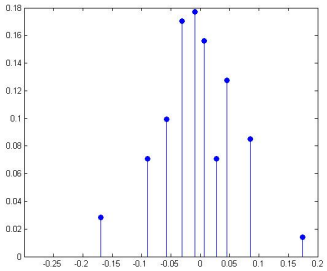

Figure 6.4: Representative days for ΔWG between 6^{th} and 12^{th} hours in February, with their correspondent frequency percentage (y axis)

July In figures 6.7 and 6.8 the 10 representative days, each with it's percentage[5] value, are presented, both for WG production in hour 6 and for difference in WG production between 6^{th} and 12^{th} hours respectively.

In figure 6.9 the historical cumulative density function for normalized WG production in hour 6 in July (blue line) is plotted with the one coming out from the distribution of representing days (red line); also representing days are indicated (yellow dots). The mean quadratic error between the two curves is 0.07%, that is the match between the two curves is very good.

In figure 6.10 the historical cumulative density function for normalized ΔWG production between 6^{th} and 12^{th} hours in July (blue line) is plotted with the one coming out from the distribution of representing days (red line); also representative days are indicated (yellow dots). Since the mean quadratic error between the two curves is 0.07%, it can be said again that the match between the two curves is very good.

[5]Again calculated as the relative frequency of occurrence

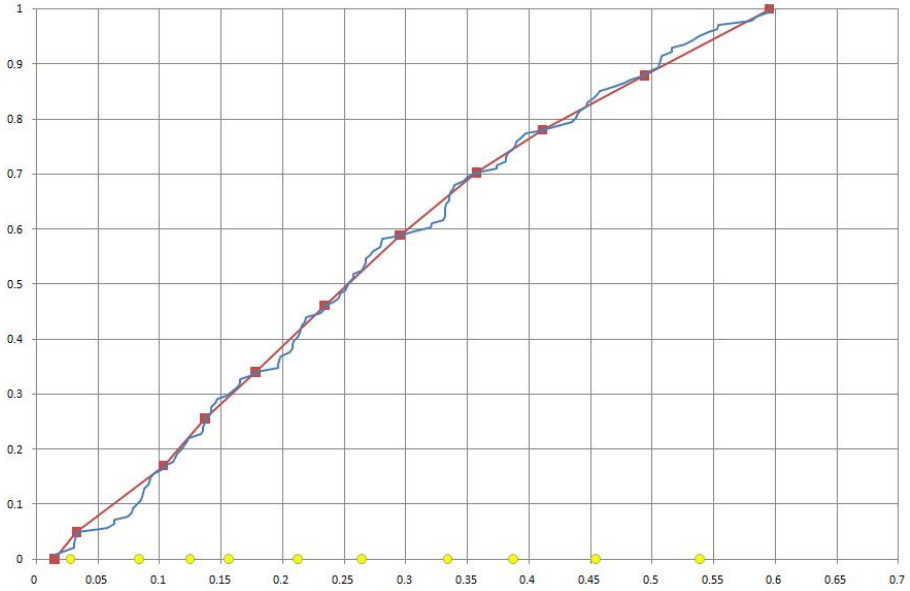

Figure 6.5: Cumulative density function, real and approximated by introduction of representative days, of normalized WG in hour 6 in February

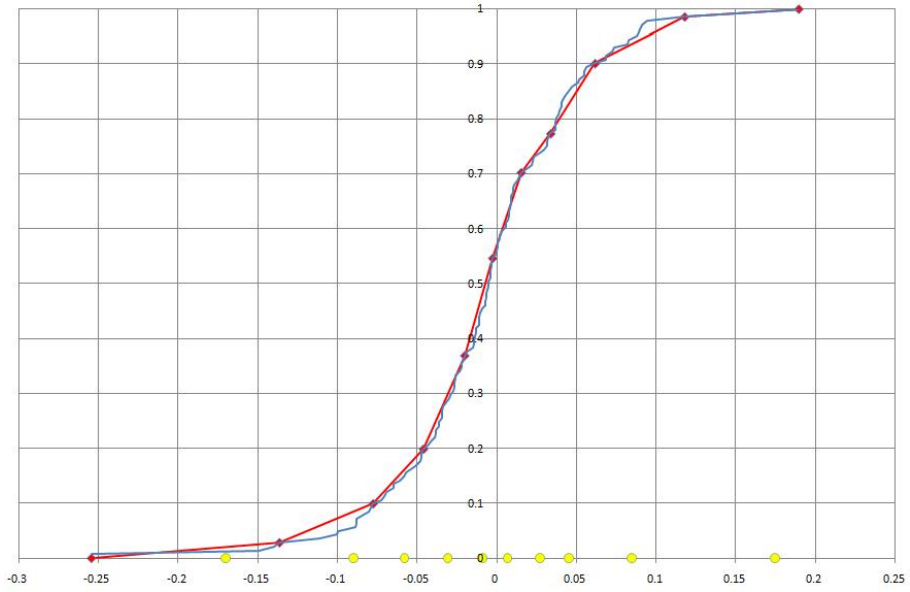

Figure 6.6: Cumulative density function, real and approximated by introduction of representative days, of normalized difference in WG between 6^{th} and 12^{th} hours in February

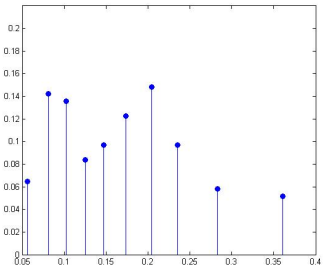

Figure 6.7: Representative days for WG in hour 6 in July, with their correspondent frequency percentage (y axis)

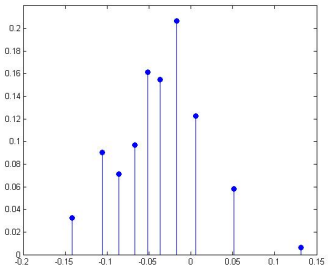

Figure 6.8: Representative days for ΔWG between 6^{th} and 12^{th} hours in February, with their correspondent frequency percentage (y axis)

6.1.2 Statistical Analysis Results

Below we present the statistical informations that can be extrapolated from the observation of WG data for the months of February and July.

February As we can see from fig. 6.6, the analysis of WG during the hours of the first increase in daily demand (i.e. from hour 6 to hour 12) gives the important result that about 55% of days shows a decrease in WG between 6^{th} and 12^{th} hours and 45% an increase; this means that the chances to encounter a (desirable) increase in WG or a (undesirable) decrease in WG are practically the same.

By fig.6.5 we can see that the cdf of WG in hour 6 shows a quite uniform tendency and that for less than 90% of the days the production does not exceed the 50% of the installed capacity and never exceeds the 60%.

July As we can see from fig. 6.10, the analysis of WG during the hours of the first increase in daily demand (i.e. from hour 6 to hour 12) gives the

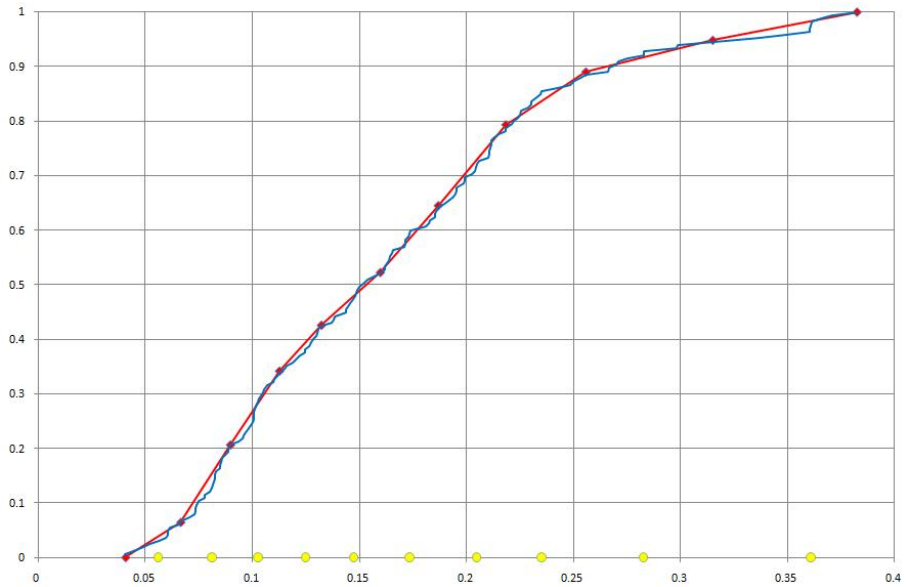

Figure 6.9: Cumulative density function of normalized WG in hour 6 in July

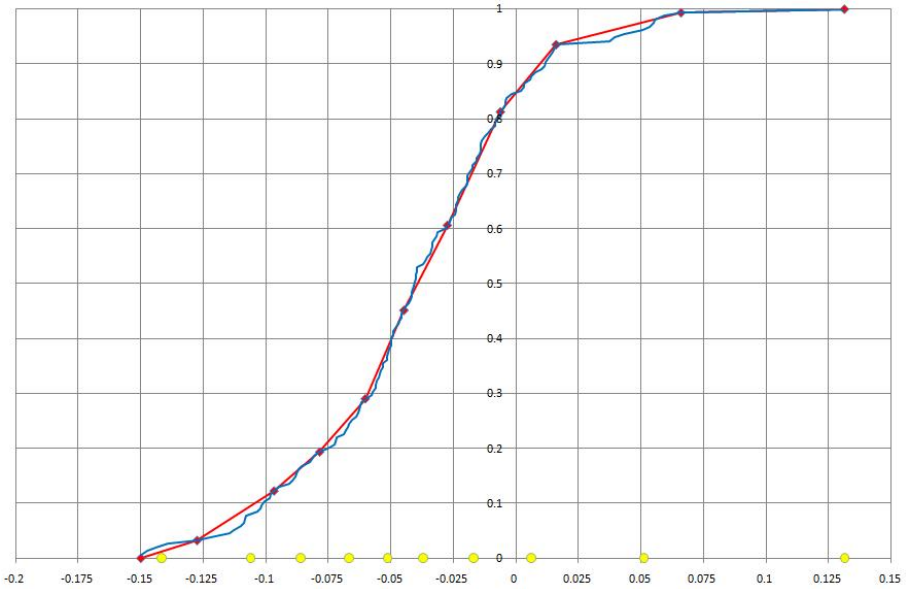

Figure 6.10: Cumulative density function, real and approximated by introduction of representative days, of normalized ΔWG between 6^{th} and 12^{th} hours in July

important result that about the 85% of the days show a decrease in WG; this implies that in July WG increases the Dem upwards ramp of the system between 6^{th} and 12^{th} hours.

By fig. 6.9 the cdf of WG in hour 6 shows a quite uniform tendency and that for more than the 85% of the days the production does not exceed the 25% of the installed capacity and never exceeds the 39%.

Chapter 7

Conclusions

In chapter 5, by means of a statistical test developed in Appendix B, we performed a classification of working days (section 5.2.1), weeks (section 5.2.2) and hours in months (section 5.2.3) and seasons (section 5.2.4) considering correlation between Dem and WG data series.

The results showed a constantly spread negative tendency in correlation during Summer, more strong in the second half of the day. This means that in Summer, and during all the day, there is a strong chance that WG will increase the upwards ramp of the system or will lead to energy spillage during hours of Dem decrease.

For the other 3 seasons no clear tendency could be individuated.

In chapter 6 we have studied, by means of cluster analysis, the behavior of WG in the months of February and July with respect to the following critical issues:

- the difference of generation between hours 6^{th} and 12^{th}
- the generation in hour 6.

Regarding the first issue, it results evident that in July the chance to find a decreasing WG simultaneously to an increasing Dem is very high. This is in complete agreement with results of Chapter 5.

A simultaneous increase in Dem and decrease in WG causes an upward ramp for production for the other generation units.

In February, on the contrary, the chance to meet decreasing or increasing WG during the upwards ramp of Dem is substantially equal (in perfect accordance with results in Chapter 5).

Other important information comes from section 6.1.1 and refers to cluster analysis itself: the representative days resulting from direct application of theory give a very good approximation of the real problem.

Chapter 8

Development of a Stochastic LP Model for the Solution of the UC Problem in Power Systems with High RES Penetration

8.1 The Unit Commitment Problem

The Unit Commitment (UC) Problem consists in defining an optimal hourly schedule for thermal and hydro generation plants. It is a large scale Mixed Integer (MI) Non-Linear Stochastic problem since it deals with integer variables (e.g. generation units status), non-linear functions (e.g. thermal generation cost functions), data affected by uncertainty (e.g. load, RES generation and fuel prices) and a large number of variables and constraints; the optimality is considered usually with respect to the minimization of total costs ([**?**]).

The uncertainty on demand is critical since units' scheduling is performed in advance (Day-Ahead Market) and a large part of thermal generation technologies (e.g. coal-fired plants) does not provide enough operational flexibility.

Non linear costs can be easily linearized, but only starting from the middle 1990's a series of works, in particular [**?**] and [14], developed solution techniques able to tackle the Stochastic Linear UC problem with a reasonable computational cost. From there on, the research on the topic flourished (for a complete review on the existing literature, refer to [15]).

Until the beginning of the 2000's the principal source of uncertainty was the demand, and the UC problem was related to test power systems' safety in supplying it and to calculate more precise reserve margins for operation ([**?**], [14], [16]).

Thus, from the beginning, the UC Problem considered situations of perfect competition markets, in which the operators aim to maximize profits (thus minimizing costs), or perfect monopoly markets, in which the operator aims to minimize costs. Real energy markets are actually far from these two models, but rather are oligopolies in which decision taking is not necessarily, and not usually, based on costs minimization. Anyway, the effort to take into account all the possible market strategies for all the operators is far too hard, mainly if the horizon is larger than the single day, and could introduce errors higher than the error introduced with the minimal costs hypothesis.

Starting from the middle 2000's, the amount of power generated by means of Renewable Energy Sources (RES) increased rapidly. Some of these sources are affected by high uncertainty and unpredictability, in particular Wind Generation (WG). Due to the fact that RES have dispatching priority, their generation must be considered as an injection of power in the system and then subtracted from the demand in order to obtain a "net" load (called "*dispatchable*" in the following chapters) upon which traditional sources compete on the market. Thus, conventional generation units face an even higher uncertainty in load and system safety becomes more critical. Large part of the

studies performed in the last years ([17], [18], [19], [20], [**?**]) are focused on this topic.

8.2 State of the Art

In power systems analysis, simulating models can be classified with respect to the simulation time horizon into three classes:

- short term, when the horizon is no longer than a few hours (usually 24 hours);
- medium term, when the time horizon goes from one week to one year;
- long term, when the time horizon is longer than one year.

Obviously, a different choice on time horizon implies also different details on the information that the results of a performed calculation can give. For further details is possible to refer to [21].

All the works analyzed in section 8.1 have a short term horizon, usually 24 hours. One of them ([**?**]) is able to analyze one whole year, but by means of coupling the results of 364 single days. This can be limiting, since for some generation technologies, the flexibility is so low that tenths of hours must be waited between consecutive status changes. Thus, at least a medium term horizon have to be considered.

The increase in the number of hours considered leads to a corresponding increase in the number of integer variables involved. The direct consequence is that the time and physical memory required to solve the MI problem become extremely large.

Since the computational complexity of the UC problem is mainly due to the presence of integer variables, one possible solution consists in the relaxation of the problem to a continuous formulation, easier to solve, coupled

to an heuristic procedure capable to determine the value of the integer variables not considered in the optimization process.

One example of this approach is the Medium Term Power System Simulator MTSIM, developed by RSE SpA (see [21]), in which the calculation of an optimal UC is performed by means of two steps:

1. a first LP optimization, in which for all existing generation units an hourly flexibility of operation is considered, calculates optimal power output;

2. a three-step heuristic procedure, receiving as input optimal power output just calculated in step 1, reintroduces all the constraints limiting flexibility of operation and calculates, for all thermal units, a UC considering economical convenience in units' operation.

Such a model, which has been used for a variety of studies on Italian and European Power Systems (see [22], [23] and [24] for some examples), is able to reduce drastically the computational complexity without penalizing too much solution optimality. But is not able to deal with uncertainty, which is strictly part of Power Systems operation.

This present work aims to create a Medium Term Power System Simulator capable to tackle uncertainty on RES power generation by introducing Stochastic Programming techniques into the existing MTSIM; the new obtained model is called s-MTISM and its mathematical formulation is described in Chapter 9.

s-MTSIM mode has been validated on simple test cases and then used on a relevant case study; all the results are showed in Chapter 10 and discussed along with all the model development process in Chapter 11.

Chapter 9

The Mathematical Model

s-MTSIM is a zonal market simulator based on Stochastic Linear Programming techniques. In this chapter its mathematical formulation is presented.

The model must be able to simulate a power system divided into different market zones (they could be different countries in a continental system as well as the sub-division of a national system, as for Italian system [25]). The aim of the model is to determine hourly the optimal Unit Commitment (UC) of thermal generation units in presence of the high degrees of uncertainty associated to the high penetration of Renewable Sources (RES) in the system itself.

Power systems are naturally affected by a certain level of uncertainty, mainly due to unexpected failure of generation devices and to non perfect predictability of demand of power. This inherent uncertainty increases highly in presence of a high penetration of RES in the system.

In facts, RES can be affected by high degrees of uncertainty, mainly due to their unpredictable nature. Wind Generation, in particular, is affected by high forecast errors. As a first consequence, for some RES, generation cannot be planned or decided in advance: it must be considered as an injection

of power in the system and has to be subtracted from the demand of the system in order to obtain a dispatchable load upon which traditional sources will compete.

It is possible to build statistical descriptions of these uncertainties and thus it is possible to build scenarios of RES generation levels and calculate for each one a corresponding probability.

Not all the thermal generation technologies suffer the effects of the high degrees of volatility of RES: if it is possible to connect or disconnect one unit hourly, then it is possible to use this *flexible* unit only when this is economically convenient. If it is not possible, that is if one thermal unit does not possess this kind of flexibility, it becomes necessary to consider the RES volatility when the use of the thermal unit is planned (UC). Due to these considerations thermal generation units can be divided into flexible and non flexible units.

In the following paragraphs it will be introduced firstly a complete Stochastic Mixed Integer Linear Programming formulation for the simulation of one electric system with different market zones and hourly detail. Then, the heuristic implementation upon which the s-MTSIM model is based will be presented.

9.1 A Stochastic MILP modelization

9.1.1 Sets

In order to describe the system which the Stochastic Mixed Integer Linear Programming model will simulate, the following sets must be introduced:

T set of hours in the simulation period, indexed by t;

G set of non flexible thermal generators, indexed by g;

F set of flexible thermal generators, indexed by f;

B set of equivalent[1] reservoir hydro plants, indexed by b;

Z set of price zones, indexed by z;

L set of connections between price zones, indexed by l;

Φ set of fuels, indexed by ϕ;

S set of scenarios, indexed by s.

For the sake of simplicity in notation, the following set is introduced:

U set of thermal generators, i.e. $U \doteq G \cup F$.

In addition, the following subsets are defined:

G_z subset of non flexible thermal generators g located in zone z;

F_z subset of flexible thermal generators f located in zone z;

B_z subset of equivalent reservoir hydro plants b located in zone z;

$\Phi(u)$ subset of fuels used in thermal unit u;

9.1.2 Decision Variables

The status of the system is described by the following *decision variables*:

- the status $\gamma_{g,t}$ of non flexible thermal unit g in hour t;
- the power output $p^G_{g,t,s}$ of non flexible thermal unit g in hour t in scenario s;
- the power output $p^F_{f,t,s}$ of flexible thermal unit f in hour t in scenario s;

[1]Hydro power plants belonging to the same producer, located in the same market zone and using the same generation technology are grouped in one equivalent plant.

- the power output $p^B_{b,t,s}$ of reservoir hydro plant b in hour t in scenario s;

- the power $q^B_{b,t,s}$ used for pumping in reservoir hydro plant b in hour t in scenario s;

- the Energy $ENP_{z,t,s}$ Not Provided to load (i.e. load shedding) in zone z in hour t in scenario s;

- the Energy $EIE_{z,t,s}$ In Excess in zone z in hour t in scenario s;

- the volume of water $v_{b,t,s}$ present in reservoir of hydro plant b in hour t in scenario s;

- the water spillage $w_{b,t,s}$ from reservoir of hydro plant b in hour t in scenario s;

- the power flow $TR_{l,t,s}$ on connection l in hour t in scenario s;

- the European Union allowances for emission trading et_s bought or sold in the whole simulated time interval in scenario s;

- the clean development mechanism credits cdm_s bought or sold in the whole simulated time interval in scenario s;

Among all the decision variables, the $\gamma_{g,t}$'s are the *first stage variables*, i.e. the variables relative to the decisions that must be taken before the actual realization of the uncertain parameter becomes known; thus, they are independent from the scenario s. All the other decision variables are *second stage variables*, meaning that their value depends on the realization of the stochastic parameter of the simulation, and so they are dependent on the scenario s.

9.1.3 Constraints

Not any status is accessible by the system under simulation, due to phisical, technical or economical limits. Mathematically this is described by means of the introduction of a number of constraints which the decision variables must satisfy. Following the constraints describing the system under analysis are introduced:

- the status $\gamma_{g,t}$ of non flexible thermal unit g in hour t must be 1 (plant on) or 0 (plant off)

$$\gamma_{g,t} \in \{0, 1\} \ ; \tag{9.1}$$

  that is, $\gamma_{g,t}$ are *integer variables*;

- if plant g in hour t is on (i.e. $\gamma_{g,t} = 1$), then the power output $p^G_{g,t,s}$ of non flexible thermal unit g in hour t in scenario s is bounded above by the maximum power output $\overline{p}^G_g$ and bounded below by the minimum power output $\underline{p}^G_g$; if plant g in hour t is off (i.e. $\gamma_{g,t} = 0$), then the power output $p^G_{g,t,s}$ of non flexible thermal unit g in hour t in scenario s must be equal to 0:

$$\gamma_{g,t} \cdot \underline{p}^G_g \ \leq \ p^G_{g,t,s} \ \leq \ \gamma_{g,t} \cdot \overline{p}^G_g \ ; \tag{9.2}$$

- the increase of power output of non flexible thermal unit g between hours $t-1$ and t in scenario s is bounded above by the technical hourly upwards ramp limit δ_g:

$$p^G_{g,t,s} - p^G_{g,t-1,s} \leq \delta_g; \tag{9.3}$$

- the power output $p^F_{f,t,s}$ of flexible thermal unit g in hour t in scenario s is non-negative and bounded above by the maximum power output $\overline{p}^F_f$

$$0 \ \leq \ p^F_{f,t,s} \ \leq \ \overline{p}^F_f \ ; \tag{9.4}$$

- the power output $p^B_{b,t,s}$ of reservoir hydro plant b in hour t in scenario s is non-negative and bounded above by the maximum power output $\overline{p}^B_b$

$$0 \ \leq \ p^B_{b,t,s} \ \leq \ \overline{p}^B_b \ ; \tag{9.5}$$

- the power $q^B_{b,t,s}$ used for pumping in reservoir hydro plant b in hour t in scenario s is non-negative and bounded above by the maximum power $\overline{q}^B_b$

$$0 \ \leq \ q^B_{b,t,s} \ \leq \ \overline{q}^B_b \ ; \tag{9.6}$$

if the equivalent hydro plant b has a pumping device, then $\overline{q}^B_b > 0$, otherwise $\overline{q}^B_b = 0$;

- the Energy $ENP_{z,t,s}$ Not Provided to load in zone z in hour t in scenario s is non negative

$$ENP_{z,t,s} \ \geq \ 0; \tag{9.7}$$

- the Energy $EIE_{z,t,s}$ In Excess in zone z in hour t in scenario s is non negative

$$EIE_{z,t,s} \ \geq \ 0; \tag{9.8}$$

- the volume of water $v_{b,t,s}$ present in reservoir of hydro plant b in hour t in scenario s is bounded above by the maximum volume of water available for reservoir b $\overline{v}_b$ and bounded below by the minimum volume of water available for reservoir b $\underline{v}_b$

$$\underline{v}_b \ \leq \ v_{b,t,s} \ \leq \ \overline{v}_b \ ; \tag{9.9}$$

$v_{b,t,s}$ is defined by the following equation:

$$v_{b,t,s} = v_{b,t-1,s} + n_{b,t} - w_{b,t,s} - \Delta t_t \left(\frac{p^B_{b,t,s}}{\lambda_b} + \frac{\eta_b \cdot q^B_{b,t,s}}{\lambda_b} \right), \tag{9.10}$$

where $n_{b,t}$ are the natural inflows into reservoir b at hour t, Δt_t is the length of the time discretization interval t, λ_b is a conversion factor between energy and volume units and η_b is the pumping efficiency for reservoir b;

- the water spillage $w_{b,t,s}$ from reservoir of hydro plant b in hour t in scenario s is non-negative and bounded above by the maximum water spillage for reservoir b $\overline{w}_b$

$$0 \ \leq \ w_{b,t,s} \ \leq \ \overline{w}_b \ ; \tag{9.11}$$

- the EU allowances for emission trading et_s bought or sold in the whole simulated time interval in scenario s is bounded above by the maximum amount of allowances which can be bought $\overline{et}$ and bounded below by the maximum amount of allowances that can be sold $\underline{et}$, which is negative by convention

$$\underline{et} \;\leq\; et_s \;\leq\; \overline{et}\;; \tag{9.12}$$

- the clean development mechanism credits cdm_s bought or sold in the whole simulated time interval in scenario s is bounded above by the maximum amount of credits which can be bought $\overline{cdm}$ and bounded below by the maximum amount of credits which can be sold $\underline{cdm}$, which is negative by convention

$$\underline{cdm} \;\leq\; cdm_s \;\leq\; \overline{cdm}\;; \tag{9.13}$$

- if the non flexible thermal unit g is started up in hour t, it must be kept on either for the minimum up time t_g^u, if $t + t_g^u - 1 \leq |T|$, or until the last hour $|T|$ of the planning period, otherwise; therefore the minimum up time constraint is

$$\sum_{\tau=t+1}^{t+\hat{t}_g^u} \gamma_{g,\tau} \geq \hat{t}_g^u \cdot (\gamma_{g,t} - \gamma_{g,t-1}) \tag{9.14}$$

  with $\hat{t}_g^u = \min\left(t_g^u - 1, |T| - t\right)$;

- if non flexible thermal unit g is shut down in hour t, it must be kept off either for the minimum down time t_g^d, if $t + t_g^d - 1 \leq |T|$, or until the last hour $|T|$ of the planning period, otherwise; therefore the minimum down time constraint is

$$\sum_{\tau=t+1}^{t+\hat{t}_g^d} (1 - \gamma_{g,\tau}) \geq \hat{t}_g^d \cdot (\gamma_{g,t-1} - \gamma_{g,t}) \tag{9.15}$$

  with $\hat{t}_g^d = \min\left(t_g^d - 1, |T| - t\right)$;

- the energy balance constraint in hour t in scenario s must be satisfied

$$\Delta t_t \left[\sum_{g\in G} p^G_{g,t,s} + \sum_{f\in F} p^F_{f,t,s} + \sum_{b\in B} \left(p^B_{b,t,s} - q^B_{b,t,s}\right)\right] = \sum_{z\in Z} \left(L_{z,t,s} - ENP_{z,t,s} + EIE_{z,t,s}\right) \tag{9.16}$$

  where $L_{z,t,s}$ denotes the "dispatchable" load in zone z in hour t in scenario s on which traditional generation units will compete on the market, calculated by subtracting the power generated by non traditional sources from the total hourly zonal load; thus, the scenarios of RES generation become scenarios of this "dispatchable" load;

- as a safety measure for the system, in order to cover unexpected failures in generation, it is usually prescribed that in zone z in hour t non flexible thermal units which status is on, flexible thermal units and hydro power plants must be able, if needed, to provide additional power generation at least equal to a fraction $R_{z,t}$, comprehensive of all reserve terms in zone z, of the total zonal load:

$$\sum_{g\in G_z} \gamma_{g,t} \left(\overline{p}^G_g - p^G_{g,t,s}\right) + \sum_{f\in F_z} \left(\overline{p}^F_f - p^F_{f,t,s}\right) + + \sum_{b\in B_z} \left(\overline{p}^B_b - p^B_{b,t,s}\right) \geq R_{z,t}; \tag{9.17}$$

- the power flow $TR_{l,t,s}$ on connection l in hour t in scenario s is defined by:

$$TR_{l,t,s} = \sum_{z\in Z} \sigma_{l,z} \left\{\Delta t_t \left[\sum_{g\in G_z} p^G_{g,t,s} + \sum_{f\in F_z} p^F_{f,t,s} + + \sum_{b\in B_z} \left(p^B_{b,t,s} - q^B_{b,t,s}\right)\right] - L_{z,t,s} + ENP_{z,t,s} - EIE_{z,t,s}\right\}. \tag{9.18}$$

  Here, the coefficients $\sigma_{l,z}$ represent the Power Transfer Distribution Factors (ptdf) and express the percentage of a power transfer from source A to sink B that flows on each transmission facility that is part of the connection between A and B.
  Each variable $TR_{l,t,s}$ is bounded above and below by the thermal limits

$\overline{TR}_{l,t}$, positive, and $\underline{TR}_{l,t}$, negative, whose sign depends on the convention decided for the transmission line direction:

$$\underline{TR}_{l,t} \;\leq\; TR_{l,t,s} \;\leq\; \overline{TR}_{l,t}; \tag{9.19}$$

- the total amount of CO_2 emissions in scenario s must be lower than the system limit $\overline{PCO_2}$:

$$\sum_{t\in T}\left[\sum_{g\in G}\sum_{\phi\in\Phi(g)}\pi_{g,t,\phi}f_{CO_2,\phi}\left(B_{1g,t,\phi}p^G_{g,t,s}+B_{0g,t,\phi}\gamma_{g,t}\right)+\right.$$
$$\left.\sum_{f\in F}\sum_{\phi\in\Phi(f)}\pi_{f,t,\phi}f_{CO_2,\phi}\left(B_{1f,t,\phi}p^F_{f,t,s}\right)\right]\leq\overline{PCO_2}+et_s+cdm_s \tag{9.20}$$

  where $\pi_{g,t,\phi}$ or $\pi_{f,t,\phi}$ is the fraction of power generated by the considered thermal unit by means of fuel ϕ in hour t, $f_{CO_2,\phi}$ is the CO_2 emission coefficient for the fuel ϕ and the terms $B_{1g,t,\phi}$, $B_{0g,t,\phi}$ and $B_{1f,t,\phi}$ describe the linear consumption curves for the non flexible plant g and the flexible plant f respectively in hour t, as defined in section C.1.

9.1.4 Objective Function

Among all solutions that satisfy constraints (9.1) to (9.20), one must be determined that minimizes the annual generation cost[2], which is the sum of the following terms:

- fuel costs and variable costs of thermal units;
- the cost of Energy In Excess;
- the cost of Energy Not Produced;

[2]A market simulator should minimize market prices; anyway, since the beginning (refer to [**?**]), the solution of the UC problem has had the minimization of costs as its o.f.; furthermore, in s-MTSIM it is possible to include among the costs for each generation plant a term indicating, if existing, its strategy of offering on market.

- the costs of emission certificates trading.

For what concerns costs depending on scenarios, the corresponding therms in the formulation are weighted by the corresponding scenario probability ψ_s.

The total cost for the system in the whole simulation time interval is thus expressed by the objective function

$$\begin{aligned} &\textstyle\sum_{t\in T}\left\{\sum_{g\in G}\left[\sum_{\phi\in\Phi(g)}\left(\pi_{g,t,\phi}C_{\phi,t}B_{0g,t,\phi}\right)\gamma_{g,t}\right]+\right. \\ &+\textstyle\sum_{s\in S}\psi_s\left[\Delta t_t\left(\sum_{g\in G}c_{g,t}p^G_{g,t,s}+\sum_{f\in F}c_{f,t}p^F_{f,t,s}\right)+\right. \\ &\left.\left.+\textstyle\sum_{z\in Z}\left(VOLL\cdot ENP_{z,t,s}+VOEE\cdot EIE_{z,t,s}\right)+c_{et}et_s+c_{cdm}cdm_s\right]\right\} \end{aligned} \tag{9.21}$$

where:

- $C_{\phi,t}$ is the price of fuel ϕ in hour t, expressed in [€/GJ][3];
- $c_{u,t}$ is the variable cost per MWh produced ([€/MWh]), for thermal unit u in hour t;
- $VOLL$ is the Value Of Lost Load [€/MWh];
- $VOEE$ is the Value Of Exceeding Energy [€/MWh];
- c_{et} is the EU allowance et price expressed in [€/t$_{CO_2}$];
- c_{cdm} is the cdm credit price expressed in [€/t$_{CO_2}$].

Variable cost $c_{u,t}$ is defined by different terms, as follows:

$$c_{u,t}=A_{u,t}+BU_{u,t}+ECO_{2u,t}+ENO_{xu,t}+var_{u,t} \tag{9.22}$$

where:

- $A_{u,t}$ represents fuel consumption cost for plant u in hour t and is defined by:

$$A_{u,t}=\sum_{\phi\in\Phi(u)}\left(\pi_{u,t,\phi}C_{\phi,t}B_{1u,t,\phi}\right);$$

[3]Fuel consumption is expressed as the amount of thermal energy, obtained by burning fuel ϕ, needed to produce an electric power output $p_{u,t,s}$, as explained in appendix C

- $BU_{u,t}$ represents the Bid-Up strategy, if any, for plant u in hour t;
- $ECO_{2u,t}$ represents the costs due to CO_2 emission for plant u in hour t and is defined as:

$$ECO_{2u,t} = C_{CO_2} \sum_{\phi \in \Phi(u)} \left(\pi_{u,t,\phi} f_{CO_2 \phi} B_{1u,t,\phi} \right),$$

  where C_{CO_2} is the price for emitting $1t$ of CO_2;
- $ENO_{xu,t}$ represents the costs due to polluting emissions other than CO_2 for plant u in hour t and is defined as:

$$ENO_{xu,t} = f_{NO_x u} \cdot C_{NO_x},$$

  where $f_{NO_x u}$ is the specific polluting emission factor for plant u and C_{NO_x} is the price for emitting $1t$ of polluting gas;
- $var_{u,t}$ represents other variable costs for plant u in hour t.

9.1.5 Simulation Data and Stochastic Term

The upper and lower bounds terms, introduced in the definition of the constraints in paragraph 9.1.3, describe the system under analysis and so they are external data.

Furthermore, in the description of the model there are other terms describing the conditions under which the system is analyzed and thus must be external data:

- the costs in the objective function ($VOLL$, $VOEE$ and all the right-hand-side terms in equation (9.22));
- the "dispatchable" load $L_{z,t,s}$;
- the natural water inflows in hydro reservoirs.

The input structure is described in Chapter **??**.

9.1.6 Results of the Model

The Stochastic MILP model described in previous sections gives as results the definition of a UC calculated considering the uncertainty on RES generation but does not give any indication about how conventional generation units have to be dispatched, since this depends on the actual realization of the RES generation.

Thus, another optimization step is needed, which considers as input the UC just calculated and only one RES generation profile, that profile representing RES actual realization (which can be one of the scenarios profiles considered in the Stochastic model as well as a completely new one).

This new step is the deterministic version of the model described in the previous sections, with the following differences:

- only one scenario is considered, the one referred to the actual realization of RES power generation;
- $\gamma_{g,t}^{G}$ are taken as input from the results of the Stochastic model, then the constraints 9.1 are no more considered;
- similarly, constraints 9.14 and 9.15 are no more considered since they have been already taken into account in the definition of the UC.

Among the most important results coming out from this deterministic step there are:

- the optimal dispatching of all the traditional generation units (thermal and hydro);
- the total costs for the System;
- the hourly power exchange between market zones;
- the total fuel consumption;

- the total polluting emissions;

- the hourly zonal prices, calculated as showed in appendix D.

9.1.7 Computational Cost

In order to evaluate the computational and memory cost that the solution of such a Stochastic MILP model would require, an estimation of the number of variables involved is here presented, starting from the evaluation of the number of elements in each category of structures present in the system. For instance, in our modelization of the Italian power system (for an example refer to [24]):

- non flexible thermal units: ~ 160;

- flexible thermal units ~ 40;

- equivalent hydro power plants ~ 30;

- market zones 11 (see [25]);

- connection lines 10;

thus, even considering only the simulation of a week, i.e. 168 hours, with 5 RES scenarios, we obtain that the simulation would have to calculate the value of 322000 variables, of which about 27000 are integer. If we consider one whole year these numbers increase respectively to about 16820000 variables, about 1400000 of which integer.

This easy calculations lead to the consideration that an heuristic formulation is needed in which integer variables are not considered. This non-integer formulation will be presented in the following sections.

9.2 The Stochastic Linear Programming Continuous Formulation for the s-MTSIM model

As discussed in section 9.1.7, a Mixed Integer formulation for s-MTSIM model would have a computational and memory costs far too large. The simplest solution would be to introduce a continuos formulation for the problem considered, that is without integer variables. Since the aim of the model is to calculate the UC for non flexible thermal units, that is exactly the values of the integer variables $\gamma_{g,t}$ that will be no more considered, it will be necessary to define an *ad hoc* procedure.

This procedure is performed with two step:

1. the first step is a Stochastic LP continuous relaxation of the MILP model presented in previous sections, in which the first stage variables are the power output $p^G_{g,t}$ of non flexible thermal unit g in hour t; the differences between the continuous and the MI formulation will be described in the following sections;

2. the second step is an heuristic procedure which defines the status $\gamma_{g,t}$ of the non flexible plants starting from the $p^G_{g,t}$ calculated by the continuous Stochastic LP model by reintroducing the constraints that were relaxed, modified or not considered.

Following, the description of these steps is presented.

9.2.1 The Stochastic LP step

The continuous Stochastic LP model for the s-MTSIM market simulator, here presented, is a reformulation of the Stochastic MILP model discussed along section 9.1. A large part of the modelization already discussed above is not affected by this reformulation, thus in the following only the differences introduced in order to transform the integer model into a continuous one are

dicussed.

The sets introduced in section 9.1.1 and their indicizations will not be modified.

On the contrary, substantial differences exist in the decision variables; here are the differences introduced with respect to what described in section 9.1.2:

- the status $\gamma_{g,t}$ of the non flexible thermal unit g in hour t is no more considered;
- the power outputs of non flexible thermal units are now the first stage variables, that is, no more depending on the scenario s; thus, the decision variable now considered is the power output $p^G_{g,t}$ of non flexible thermal unit g in hour t;
- a new variable is introduced in order to define the contribution of non flexible thermal units to the reserve: the power $\Delta p_{g,t,s}$ made available for the power reserve by non flexible thermal unit g in hour t in scenario s.

The absence of the integer variables $\gamma_{g,t}$ affects also the following constraints:

- equations (9.1), (9.14) and (9.15) can no more be considered;
- a constraint of the form (9.2) with $\underline{p}^G_g > 0$ can not be considered anymore, since it would imply that non flexible thermal units could never be turned off; so, it is no more possible to consider a minimum $\underline{p}^G_g$ for the power output $p^G_{g,t}$ of non flexible thermal unit g in hour t; the constraints (9.2) are thus reformulated as:

$$0 \;\leq\; p^G_{g,t} \;\leq\; \overline{p}^G_g \;; \tag{9.23}$$

  as a side effect of neglecting $\underline{p}^G_g$, also the consumption curves for non flexible units have to be reformulated, as described in section C.2.

- the power $\Delta p_{g,t,s}$, made available for reserve by non flexible thermal unit g in hour t in scenario s must be non negative:

$$\Delta p_{g,t,s} \geq 0; \tag{9.24}$$

the unit g can never generate a power output greater than $\overline{g}^G_{g,t}$:

$$p^G_{g,t} + \Delta p_{g,t,s} \leq \overline{p}^G_g; \tag{9.25}$$

the increase in power generation for unit g between hour $t-1$ and t can never exceed the ramp limit (see constr. (9.3)):

$$\Delta p_{g,t,s} \leq \left(p^G_{g,t-1} + \delta_g\right) - p^G_{g,t}; \tag{9.26}$$

the unit g can contribute to reserve only when it is functioning, that is $\Delta p_{g,t,s}$ must be equal to 0 when $p^G_{g,t} = 0$; a constraint of the kind $\Delta p_{g,t,s} \leq \alpha p^G_{g,t}$ in conjunction with constraint (9.24) will force exactly $\Delta p^G_{g,t,s} = 0$ when $p^G_{g,t} = 0$; in order to avoid this constraint to be more restrictive than constraint (9.25) we chose

$$\alpha = \left(\frac{\overline{p}^G_g}{\underline{p}^G_g} - 1\right)$$

so that the considered constraint will take the form:

$$p^G_{g,t} + \Delta p_{g,t,s} \leq \left(\frac{\overline{p}^G_g}{\underline{p}^G_g}\right) p^G_{g,t}; \tag{9.27}$$

in fact, when $p^G_{g,t} \geq \underline{p}^G_g$ the right-hand-side in (9.27) is greater than the right-hand-side in (9.25); when $p^G_{g,t} \leq \underline{p}^G_g$, anyway, (9.27) becomes effectively more restricting than (9.25) but in this way it is possible to reduce the error of overestimation[4] of the reserve in zone z in hour t in scenario s;

[4]In this continuous formulation an overestimation of the reserve is possible: in fact, if unit's status could be considered, unit g could never produce less than $\underline{p}^G_g$; then, $p^G_{g,t} \leq \underline{p}^G_g$ could also mean that the unit should be turned off, in which case there would be no contribution to reserve; this mathematical trick contributes in reducing the error in evaluation of reserve.

- the energy balance constraint in hour t in scenario s is rewritten as:

$$\Delta t_t \left[\sum_{g\in G} p^G_{g,t} + \sum_{f\in F} p^F_{f,t,s} + \sum_{b\in B}\left(p^B_{b,t,s} - q^B_{b,t,s}\right)\right] = \sum_{z\in Z}\left(L_{z,t,s} - ENP_{z,t,s} + EIE_{z,t,s}\right); \tag{9.28}$$

- the reserve constraint, due to the introduction of variable $\Delta p_{g,t,s}$ becomes:

$$\sum_{g\in z}\Delta p_{g,t,s} + \sum_{f\in F_z}\left(\overline{p}^F_f - p^F_{f,t,s}\right) + \sum_{b\in B_z}\left(\overline{p}^B_b - p^B_{b,t,s}\right) \geq R_{z,t}; \tag{9.29}$$

- the constraint (9.20) limiting the total amount of CO_2 emissions in scenario s, is rewritten as follows:

$$\sum_{t\in T}\left[\sum_{g\in G}\sum_{\phi\in\Phi(g)}\pi_{g,t,\phi} f_{CO_2,\phi}\hat{B}_{1g,t,\phi} p^G_{g,t} + \sum_{f\in F}\sum_{\phi\in\Phi(f)}\pi_{f,t,\phi} f_{CO_2,\phi} B_{1f,t,\phi} p^F_{f,t,s}\right] \leq \overline{PCO_2} + et_s + cdm_s, \tag{9.30}$$

  considering the introduction of the new linear consumption curve.

The objective function, which expresses the annual total cost for the system, is modified by the introduction of the new first stage variables $p^G_{g,t}$ in place of the $\gamma^G_{g,t}$'s and by the definition of the modified consumption curve for non flexible thermal units. The new objective function is:

$$\sum_{t\in T}\left\{\Delta t_t \sum_{g\in G} c_{g,t} p^G_{g,t} + \sum_{s\in S}\psi_s\left[\Delta t_t \sum_{f\in F} c_{f,t} p^F_{f,t,s} + \right.\right. \tag{9.31}$$
$$\left.\left. + \sum_{z\in Z}\left(VOLL\cdot ENP_{z,t,s} + VOEE\cdot EIE_{z,t,s}\right) + c_{et} et_s + c_{cdm} cdm_s\right]\right\}$$

where all therms are defined as in section 9.1.4, except for the term $B_{1g,t,\phi}$ which is now substituted by the linear therm of the modified consumption curve, $\hat{B}_{1g,t,\phi}$.

Input data for the Stochastic LP model are the same introduced in paragraph 9.1.5, as well as the definition of the "dispatchable" load $L_{z,t,s}$ as the stochastic parameter of the model.

9.2.2 Heuristic Calculation of UC for Non Flexible Thermal Units

The Stochastic LP model discussed in section 9.2.1 calculates the power $p^G_{g,t}$ generated by each non flexible thermal unit g in hour t, but no UC is defined: this is the aim of the stochastic procedure described in this section.

Along with $p^G_{g,t}$'s, also the average hourly zonal prices $\overline{\overline{\psi}}_{z,t}$ are necessary to the following calculations; they are calculated as the weighted average of the hourly zonal prices $\psi_{z,t,s}$ for each RES generation scenario s as follows (see also appendix D):

$$\overline{\overline{\psi}}_{z,t} = \sum_{s \in S} \psi_{z,t,s} = \sum_{s \in S} \left[\lambda^P_{t,s} + \sum_{l \in L} \sigma_{l,z} \cdot \lambda^{TR}_{l,t,s} \right], \tag{9.32}$$

where $\lambda^P_{t,s}$ are the lagrangian multipliers for constraints (9.28) and $\lambda^{TR}_{l,t,s}$ are the lagrangian multipliers for constraints (9.19).

Furthermore, in this model constraints (9.14) and (9.15) are not considered and constraints (9.2) are relaxed to the form (9.23) setting to 0 the lower bounds of flexible thermal units power generation. In order to calculate a UC which takes into account also the above-mentioned omitted constraints a three-step heuristic procedure is introduced as follows:

1. for each non flexible thermal unit g a power output threshold is defined as a fraction β of its minimum power output:

$$\underline{p}^{TH}_g = \beta \underline{p}^G_g; \tag{9.33}$$

   then for each non flexible thermal unit g in each hour t a new parameter $\hat{\gamma}_{g,t}$, representing unit g status in hour t, is introduced and $\forall (g,t)$:

$$\begin{aligned} p^G_{g,t} \geq \underline{p}^{TH}_g &\implies \hat{\gamma}_{g,t} = 1, \\ p^G_{g,t} < \underline{p}^{TH}_g &\implies \hat{\gamma}_{g,t} = 0; \end{aligned} \tag{9.34}$$

2. this step reintroduces constraints (9.14), which impose that when unit g is turned on, it must remain in this status for at least a number of consecutive hours equal to t_g^a; intervals of the kind $\Delta T_{on} = [t_a, t_b]$ such that $\forall t \in \Delta T_{on}\ \hat{\gamma}_{g,t} = 1$ are considered; when one interval ΔT_{on} which length is shorter than t_g^a is found, new intervals $\Delta \hat{T}_i = \left[\hat{t}_a, \hat{t}_b\right]$ are built adding to ΔT_{on} adjacent hours in order to reach the correct length; that means that $\forall i \Delta T_{on} \subset \Delta \hat{T}_i$; each one of these new intervals $\Delta \hat{T}_i$ is thus analyzed in order to find out if there exists an economical convenience, expressed by means of a lower bound $\underline{E}$[5] for energy produced, in keeping the unit on for all the hours in $\Delta \hat{T}$; three possible situation may happen:

   - in none of the intervals $\Delta \hat{T}_i$ it is convenient to keep the plant on, that is:
   $$\forall i \sum_{t \in \Delta \hat{T}_i} t \cdot p_{g,t}^G < \underline{E};$$
   in this case the unit is set to off in all the hours in the interval ΔT_{on}:
   $$\forall t \in \Delta T_{on}\ \hat{\gamma}_{g,t} = 0;$$

   - only in one interval $\Delta \hat{T}_i$ it is convenient to keep the plat on, that is:
   $$\exists!\ i \text{ s.t. } \sum_{t \in \Delta \hat{T}_i} t \cdot p_{g,t}^G \geq \underline{E};$$
   in this case the unit is set to on in all the hours in the interval $\Delta \hat{T}_i$:
   $$\forall t \in \Delta \hat{T}_i\ \hat{\gamma}_{g,t} = 1;$$

   - for more than one of the intervals is convenient to keep the unit g on, that is:
   $$\sum_{t \in \Delta \hat{T}_i} t \cdot p_{g,t}^G \geq \underline{E} \text{ for some } i;$$

[5] It is possible to define $\underline{E}$ in many different ways; usually, $\underline{E} = N_g \cdot \overline{p}_g^G$, with N_g an integer parameter defined by the user.

only one interval can be considered: it is chosen the interval $\Delta\hat{T}_I$ for which the profit, calculated as $\Psi_i = \sum_{t\in\Delta\hat{T}_i} \Delta t_t \left(p^G_{g,t} \cdot \overline{\overline{\psi}}_{z,t}\right)$, is maximized; then, the unit g is set to on in all the hours in the interval $\Delta\hat{T}_I$:

$$\Psi_I = \max_i \Psi_i \Longrightarrow \forall t \in \Delta\hat{T}_I \ \hat{\gamma}_{g,t} = 1;$$

3. this step reintroduces the constraints (9.15), which prescribe that when unit g is turned off, it must remain off for a number of consecutive hours at least equal to t^s_g; thus, all intervals of the kind $\Delta T^i_{off} = [t^i_c, t^i_d]$ s.t. $\forall t \in \Delta T^i_{off} \ \hat{\gamma}_{g,t} = 0$ are considered: when an interval of this kind is found whose length is shorter than the one imposed, then in all the hours of the interval the status is set to on:

$$\text{if } \left(t^i_d - t^i_c + 1\right) < t^s_g \Longrightarrow \forall t \in \Delta T^i_{off} \ \hat{\gamma}_{g,t} = 1.$$

The parameters $\hat{\gamma}_{g,t}$ defined by the procedure described above, constitute a UC for non flexible thermal plants. Due to step number 2, the calculated UC respects the principles of economical convenience that drive decision taking when planning generation units functioning; as a comment to step number 3, it can be underlined that the procedure "prefers" to keep plant on instead of turning them off, then it should be more likely to find out excess of energy rather than energy not produced, thus gaining in system safety[6].

9.2.3 A Deterministic LP Step

As for the MI model described along section 9.1, the procedure presented in sections 9.2.1 and 9.2.2 gives as results the definition of a UC calculated considering the uncertainty on RES generation but does not give any indication about how conventional generation units have to be dispatched.

Again, to complete the procedure, the deterministic LP step described

[6]Constraint on reserve could not be met in case of lack of energy.

in section 9.1.6 is needed. This step will receive as input the UC calculated by means of the procedure just described, i.e.the $\hat{\gamma}_{g,t}$'s, and one only profile for RES generation, representing actual RES realization.

9.3 Model Implementation

Even if original MTSIM model was coded in MATLAB©, the stochastic s-MTSIM model has been coded partly in GAMS© environment and partly in MATLAB©.

In particular, the stochastic LP model developed in section9.2.1 has been coded in GAMS, the choice driven by the readiness of the equation writing it allows. Anyway, since GAMS environment is not "programming oriented", preprocessing utilities and the heuristic procedure described in section 9.2.2 were coded in MATLAB.

Chapter 10

Validation Tests

10.1 Validation of Fundamentals of Stochastic Programming

When a Deterministic optimization is performed, the obtained results are optimal only for that particular parameters' value considered in the optimization process. That is, using the terminology of UC Problem theory, the UC calculated by means of a Deterministic optimization is the best only in case all the parameters of the problem have the values considered during the optimization process. If any of these parameters takes a different value, then the UC just calculated does not perform as optimal anymore.

If, for example, you run a Deterministic optimization thinking that a particular hourly Wind Generation profile, let's say WG_f, is going to realize, but, instead, the Wind Generation actual realization will be WG_a, then the performances of the system will be no more optimal.

For what concerns Wind Generation, due to forecast error, the realized hourly profile is usually different, not so rarely even largely different, from the expected one. Then, deterministic optimization runs the risk to perform very badly.

Stochastic optimization (refer to [26]), on the contrary, keeps into account the uncertainty of the optimization parameters and thus the solution obtained is the best **with respect to all the possible realization of the parameters affected by uncertainty**, that is it will perform quite well in all the possible situation that the system can face (obviously if they are considered in the stochasticity of the parameters).

Furthermore, and this is a fundamental of Stochastic Programming, a UC calculated considering stochasticity of WG will always perform better than a deterministic UC when facing a WG profile different from the one considered in the optimization process. This is what has been tested in the following example.

Consider a power system as follows:

- 159 non flexible thermal generators;
- 36 flexible thermal generators;
- 28 equivalent reservoir hydro plants;
- 12 price zones (7 actual zones + 5 limited production sites, refer to [25][1]) ;
- 11 connections between zones.

The aim is to dispatch hourly thermal and hydro generation devices in a complete year (8760 hours) minimizing total system generation costs. Imagine that only two possible WG profiles (source: [27]) can realize: one called Normale (represented in figure 10.1), which is expected to realize with a probability $\psi_N = 0.8$, and one called Debole (represented in figure 10.2) which is expected to realize with a probability $\psi_D = 0.2$. All other data come from

[1]In this test the price zone Nord is split into 2 zones, Nord Est and Nord Ovest

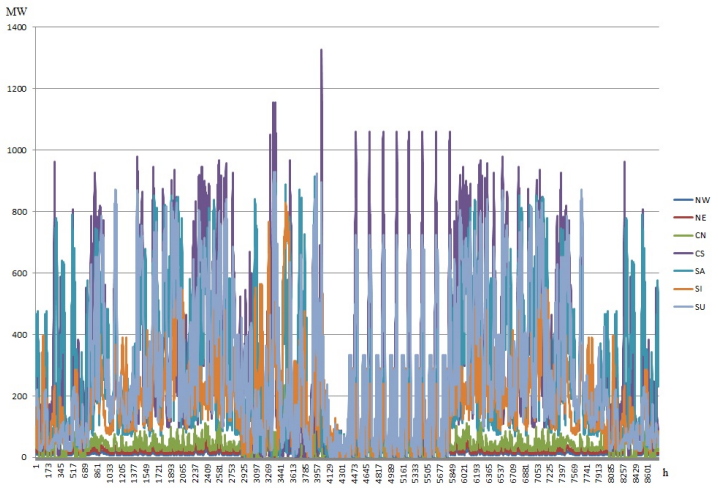

Figure 10.1: Normale WG profile - zonal and hourly detail

[28] and [29].

We want to confront the performances of the following case studies:

A the deterministic UC calculated expecting Normale profile in case of Debole profile realization;

B the stochastic UC calculated considering uncertainty on WG in case of Debole profile realization;

C the deterministic UC calculated expecting Debole profile in case of Normale profile realization;

D the stochastic UC calculated considering uncertainty on WG in case of Normale profile realization.

Results in terms of objective function and EU allowances on emission trading market are showed in table 10.1; here is possible to see that the costs that the system has to pay when the UC is calculated by means of stochastic optimization (cases B and D) are lower than when the UC is calculated

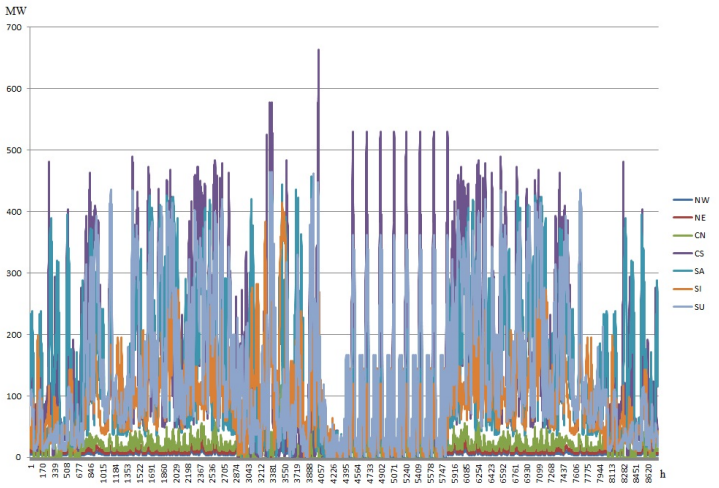

Figure 10.2: Debole WG profile - zonal and hourly detail

deterministically but faces a WG profile different from the one considered (cases A and D).

	A	B	C	D
Costs [M€]	18215	18208	17877	17816
EU CO_2 all. [Mt_{CO_2}]	22252	22209	20354	20172

Table 10.1: Results of Stochastic Optimization (B, D) vs. results of Deterministic Optimization (A, C).

10.2 Validation of the Heuristic Procedure

The solution UC_{MI} obtained by means of the MI model described in section 9.1 is surely the best possible for the UC Problem in the Power System considered. The heuristic UC_h obtained at the end of the procedure 9.2.2 is surely worse than UC_{MI}, but has the advantage to be easier to obtain.

Anyway, as it has been indicated in sections 9.1.6 and 9.2.3, the UC

obtained by means of any kind of stochastic model has to be subsequently used in a further deterministic optimization step in order to obtain the dispatch of traditional generation units in presence of the actual realization of the stochastic parameter WG.

In the following validation test, the performances of UC_{MI} and UC_h in presence of the actual realization of WG will be compared.

Consider the following power system for a one-week (i.e. 168 hours) time horizon:

- 149 non flexible thermal generators;
- 29 flexible thermal generators;
- 28 equivalent reservoir hydro plants;
- 11 price zones (6 actual zones + 5 limited production sites, refer to [25]);
- 10 connections between zones;

All costs and other data come from [28] and [29]; taking data from [27], 5 scenarios of WG profile, with zonal detail, have been considered, each with a probability $\psi_i = 0.2$.

Both the sMTSIM and the MI model have been implemented in GAMS and solved by means of CPLEX 12 solver. It must be underlined that even on a computer with 4 Intel Xeon CPU's at 2.93 GHz, 12 GB RAM and a 64-bit operative system the exact solution of the MILP model requested too much time[2]. Thus we gave up to obtain the optimum and decided to accept a sub-optimal solution: in fact, CPLEX in its solution procedure calculates a lower bound[3] for the optimum by means of relaxing the integer nature of

[2]Actually, the solution procedure was stopped after more than 10 days

[3]In this case, since its a problem of minimization.

the problem; the value of this relaxed solution is considered as the "best possible" value of the o.f. and then the quality of the solution of the MI problem is measured by means of its relative difference, in percentage and called "tolerance", with the "best possible" solution (refer to [30] for more details). It must be underlined that in this way, also the optimum will have a tolerance different from 0.

CPLEX allows to choose to stop the solution procedure when the calculated tolerance reach a decided value; we chose to consider a solution with a "tolerance" of 1%, so we substantially confronted two heuristic procedures, knowing that CPLEX solution would have been in a range of at maximum 1% from the optimum.

What appears immediately clear from table 10.2 is that computational

	$MI_{1\%}$	Heur
Objective Function [k€]	114916.3	114755.3
Computational time [s]	5243	57

Table 10.2: Performances, in terms of o.f. value and computational cost, of MI calculated UC vs. heuristically calculated UC.

cost for the heuristic procedure is of 2 orders of magnitude lower than for the MI.

As it is possible to see from table 10.2, in the considered test the heuristic procedure defined in section 9.2.2 performs even better than the MI solution with a 1% tolerance, that is the solution found by means of sMTSIM lies inside the 1% tolerance from the optimal MI solution.

In figure 10.3 hourly prices in all price zones, except for Sicily, are shown. Prices calculated by MILP model are almost always higher than prices cal-

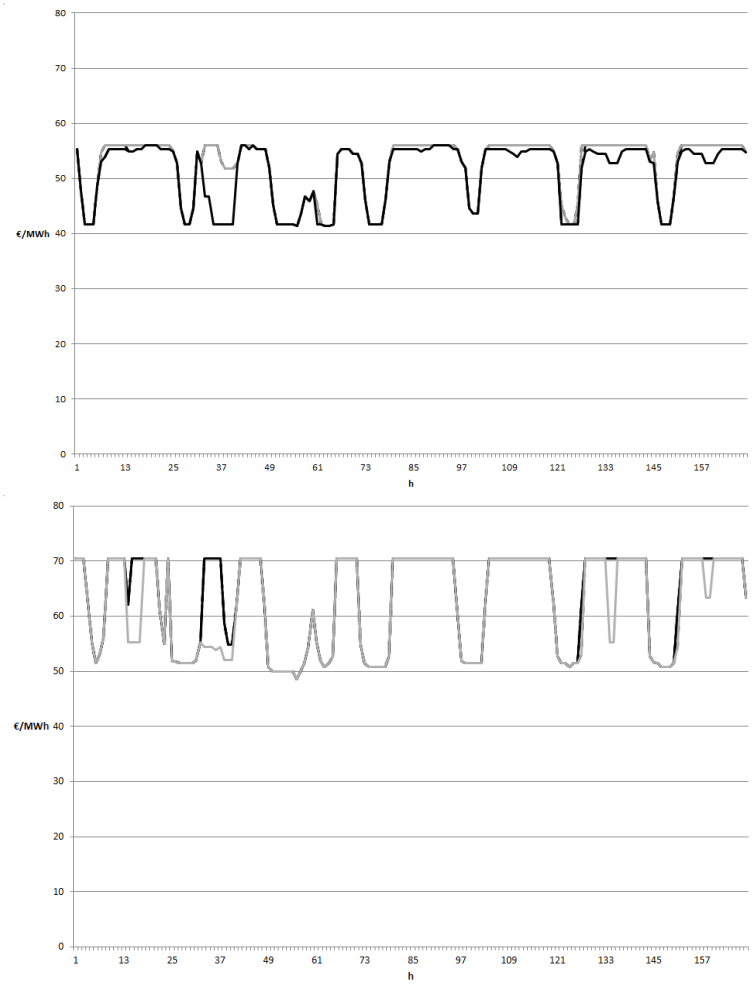

Figure 10.3: Hourly prices in other price zones calculated by sMTSIM (up) and MILP model (down)

culated by sMTSIM. This result could be explained by the tendency of the sMTSIM heuristic procedure in turning thermal units on more than turning them off. Anyway, recalling table 10.2, this does not seem to affect too much the solution with respect to objective function performances.

In figure 10.4 hourly prices in Sicily, calculated by means of sMTSIM and MILP models, are shown; we have to remark that Sicily is a price zone with

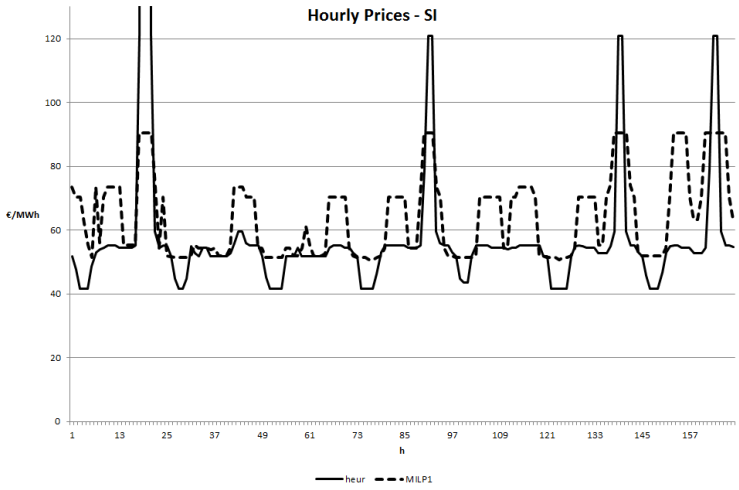

Figure 10.4: Hourly prices in Sicily resulting from sMTSIM (full line) and MILP (dashed line) model

high congestion problems on connection with other price zones and this is the reason why a lot of price peaks can be found. We can see how prices calculated by sMTISM are substantially lower from prices calculated by MILP model except for the peaks.

The reason for this is again that the heuristic procedure here introduced has the tendency to turn on plants more than to turn them off, thus there is almost always more generation capacity on line than actually needed. Furthermore, even if it comes after a LP optimization procedure, the heuristic procedure itself is based only on criterion of technical and economical convenience. Thus, it could decide to turn off plants which contribution is strongly needed but only in a couple of consecutive hours, usually the price-peack hours. As a consequence, the more expensive flexible plants need to be turned on and, as it happened in hours 19 and 20 in figure 10.4, if also the constraint on reserve (equations 9.29) is critical also a load shedding can happen.

Anyway, all the differences in prices discussed above could be conse-

	$MI_{0.65\%}$	Heur
Objective Function [k€]	114616.7	114755.3
Computational time [s]	13762	57

Table 10.3: Performances, in terms of o.f. value, of MI calculated UC vs. heuristically calculated UC.

quences of the fact that the heuristic procedure have a better performance of the MI model with the chosen tolerance of 1%. Then, we have also considered tho lower this tolerance to 0.65%: the results are showed in table 10.3 and in figures 10.5 and 10.6.

The first result is that in order to improve the MI solution of the 0.26% we increase the computational time of the 262%, one more time underlining how difficult is a MI problem to solve.

As it is possible to see, figures 10.5 and 10.6 do not differ qualitatively from figures 10.3 and 10.4, thus meaning that the differences on the prices calculated by the two models do not depend on what could be considered "the optimality level", that is the value of the objective function, but, instead, on the intrinsic difference between a pure MI model and an heuristic procedure. This validates the considerations expressed above.

It must be underlined that this is not necessarily an imperfection of the heuristic procedure. As we have discussed in section 8.1, our model is a simplification of the complexity of a real energy market, since we are describing as a *perfect competition market* what actually is an oligopoly, in which decision taking is not necessarily based on cost minimization.

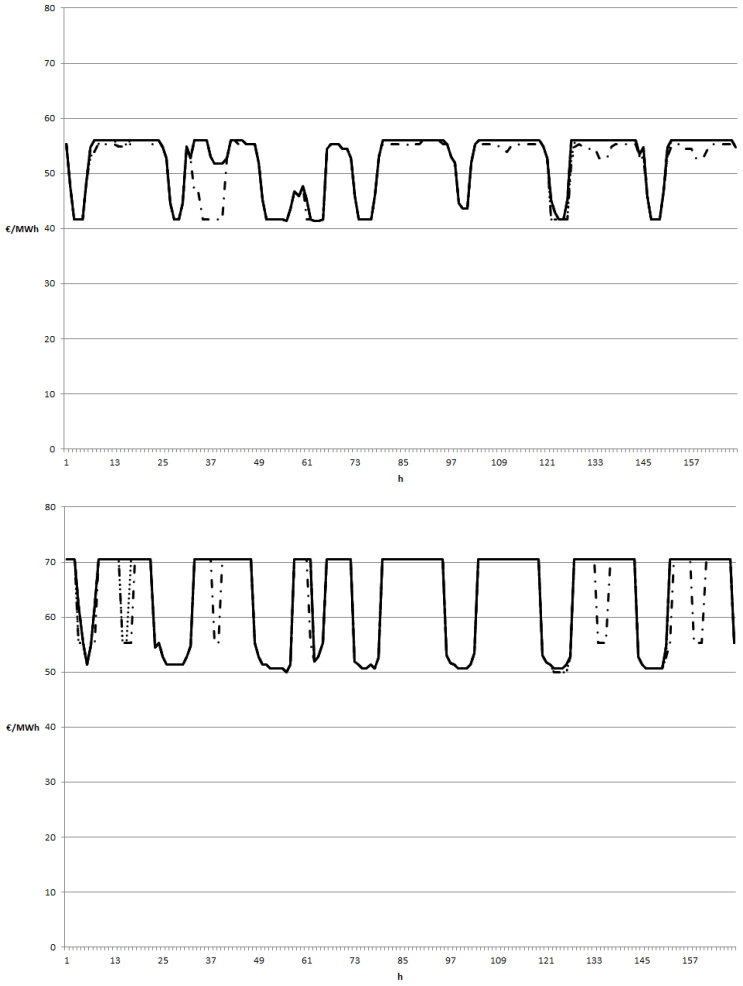

Figure 10.5: Hourly prices in other price zones calculated by sMTSIM (up) and MILP model (down)

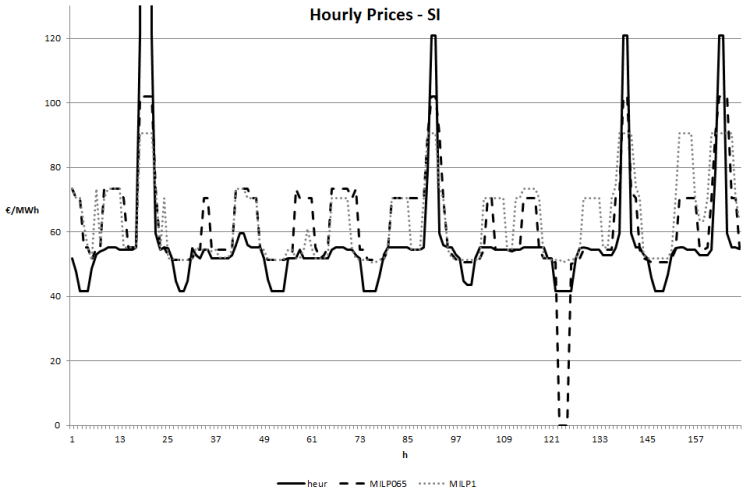

Figure 10.6: Hourly prices in Sicily resulting from sMTSIM (full line) and MILP (dashed line) model

Chapter 11

Conclusions

In this work the development of a Stochastic Programming Medium Term model is presented for the solution of the linear Unit Commitment problem in a Power System with a high RES penetration.

Unit Commitment problem has typically a large scale, stochastic, Mixed Integer nature, as discussed in section 9.1. On the other hand, for medium term time horizons the solution of the MI model of such a large scale problem has proven to be too expensive in terms of computational cost.

This is the reason why a continuous relaxation of UC problem has been proposed in section 9.2.1, along with an heuristic procedure capable of re-introducing the mixed integer nature of the problem, in section 9.2.2, as the mathematical basis for the stochastic model s-MTSIM.

The newly developed model has then been validated on a series of test cases. The first, showed in section 10.1, has proven the accordance of s-MTSIM model with Stochastic Linear Programming theory [26]. Then, in section 10.2, the heuristic procedure is compared with the MI solution for the same case in order to evaluate its influence on the optimality of the solution. In particular, this comparison underlined how the heuristic procedure

performs pretty well in terms of objective function, lying into a 1% tolerance interval around the optimal MI solution.

Furthermore, the prices resulting from the heuristic procedure showed to be lower than the ones calculated by the MI model, caused to the tendency of the heuristic to turn plants on, with the exception of the highly critical hours, due to the fact that the heuristic itself is based on mere economical and technical criterion. Anyway, both sMTSIM model and MI model try to describe by the hypothesis of perfect market (i.e. cost minimization) an oligopoly, thus resulting prices are surely not fully representative of real market prices.

Then, what really comes out from this comparison is that sMTSIM is able to reach results comparable to a MI model in a computational time largely smaller.

The remaining step is to couple sMTSIM model with a tool of RES generation analysis as like as the procedures described in chapters 2 to 7.

Appendix A

Theory of Cluster Analysis

A.1 Introduction

In statistical analysis is often useful to combine observations into groups such that each group results to be ***homogeneous*** (i.e. observations in each group result similar to each other) w.r. to certain characteristics and ***different*** from other groups w.r. to the same characteristics (i.e. observations in one group should be different from observations in other groups).

Obviously, the definition of *similarity* as like as the characteristics to be considered depend on the analysis under consideration. For example we can group people in a sample by age, sex, religion, education and whatever other else physical and psychological characteristics and also by any combination of them.

Cluster Analysis is a useful technique to perform this task. A wide and deep theorical tractation of this subject can be found in [31]. Here we are only interested in what can be helpful in our study of Demand and Wind Generation.

A.2 The Geometrical Point of View

If the sample characteristics we are taking into account are numerical in nature (height, weight or age, if we keep on with the example of the sample formed by people), we can consider any single element of the sample as a point in a n-dimensional space, where n is the number of characteristics we have to consider in building groups.

Then building groups can be seen as divide this n-dimensional spaces in k sub-spaces such that ***if a point belongs to a sub-space its distance from the other points in its same group is smaller than the distance from all the other points in the other groups.*** As an example, let's refer to the representation of the daily WG versus Dem as given in fig. 4.3-b in Chapter 4. Any day is an observation. Suppose we want to group days by means of the behavior of the curve WG versus Dem; then any observation will be a point in a 48-dimensional space, since for any of the 24 hours of the day we have to consider both the values of Demand and WG.

A.3 Distance as Measure of Similarity

The definition given above implies ***distance*** as a measure of the similarity between observations. A lot of different definitions for distance exist in mathematics and each of them has its different meaning and, thus, can be useful in different situations.

Among all the possible definitions of distance, the following two, in particular, can be useful in our analysis:

- Squared Euclidean distance

- Correlation distance.

A.3.1 Squared Euclidean Distance

If we want to categorize observations in our sample by means of n characteristics, then any observation can be considered as a point in the n-dimensional space. Then the squared euclidean distance between point i and point j is given by the following equation:

$$D_{ij} = \sum_{p=1}^{n} (X_{ip} - X_{jp})^2. \tag{A.1}$$

This is the most intuitive definition for distance and also it leads to the most intuitive way to build groups: gathering together the closest points by a geometrical point of view. Let's now underline what comes out in our specific field of analysis by using this definition for distance.

As an example, we can consider the behavior of the Dem versus WG curve between hours 6^{th} and 12^{th} in February. Any day is a point in a 14-dimensional space and in figure A.1 we can find all the points of our sample[1].

Let's divide our sample in 15 clusters by means of the Squared Euclidean distance: we already know we will obtain groups of points which will be the closest possible among any group. In figures from A.2 to A.5 we can see the 2-dimensional representation of 4 of these clusters.

Looking at figures from A.2 to A.5 we can deduce that Squared Euclidean distance creates groups in which points have a similar mean level of Demand and Wind Generation but can have a slightly different shape in the curve Dem versus WG.

[1]Which consists in all the working days in the month of February over a 5-year span

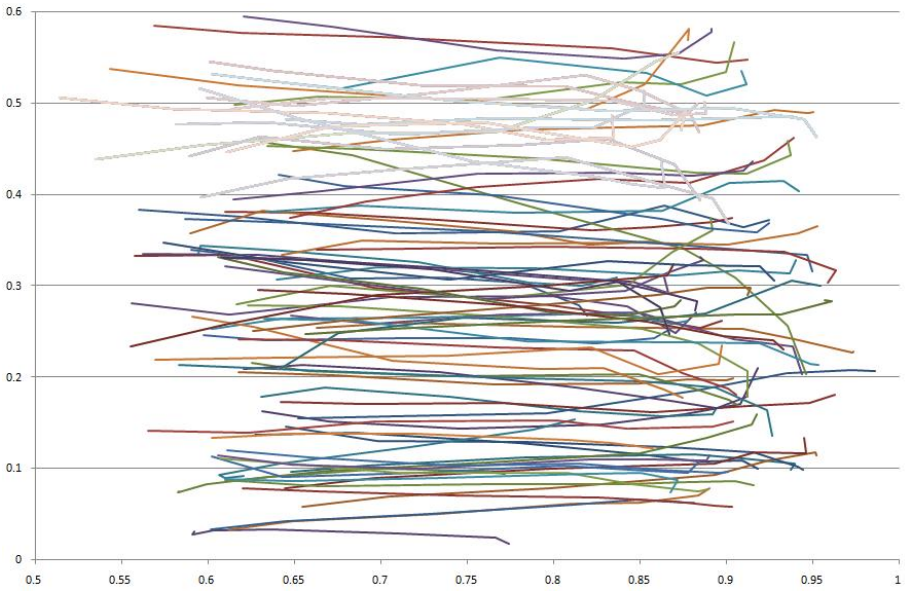

Figure A.1: Dem vs WG curve from 6.00 a.m. to 12.00 p.m. in February for different days in a 5-year span

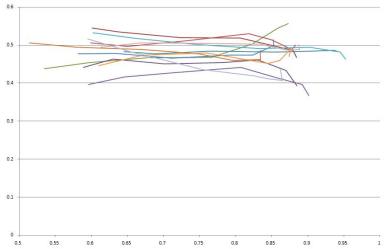

Figure A.2: Result of Cluster Analysis by means of Euclidean Distance measure - Group 1

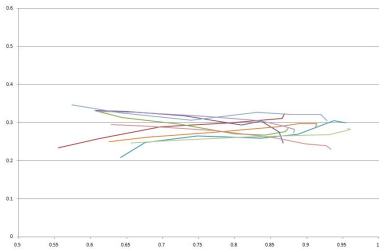

Figure A.3: Result of Cluster Analysis by means of Euclidean Distance measure - Group 2

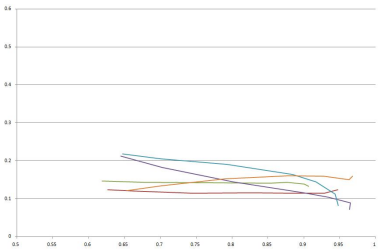

Figure A.4: Result of Cluster Analysis by means of Euclidean Distance measure - Group 3

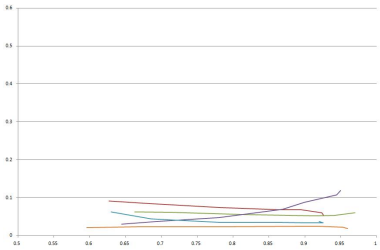

Figure A.5: Result of Cluster Analysis by means of Euclidean Distance measure - Group 4

A.3.2 Correlation Distance

In previous section we have discussed how choosing Euclidean Distance as the measure of similarity between points allows us to build clusters of points which have a similar mean level of Demand and Wind Generation but can have a slightly different shape in the curve Dem versus WG.

But we could be interested in having clusters of point with a similar shape in the curve Dem vs WG despite the level of Demand and Wind Generation. This can be obtained by using ***statistical correlation*** as a measure of similarity.

As we know from [12], *correlation* ρ is a measure of "how much" the points of 2 different series lie on a line: the closer $|\rho|$ is to 1, the more "aligned" are points. As a consequence we can define the following function

$$d_{ij} = 1 - \rho_{ij} \tag{A.2}$$

as the definition of distance between points i and j, where ρ_{ij} indicates the correlation between the two observation considered as a sequence of n values.

In figures from A.6 to A.9 are showed 4 of the 15 clusters resulting from applying the cluster analysis with correlation distance over the same sample data showed in figure A.1.

Results evident how the point in these clusters have a similar shape but a quite different level in Demand and Wind Generation.

A.4 Representative Elements

In previous paragraphs we have seen how it is possible to divide a sample in groups of similar elements. This could be useful in order to reduce the dimension of the statistical analysis, since, being all the elements of a cluster

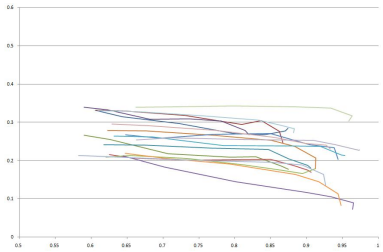

Figure A.6: Result of Cluster Analysis by means of Correlation Distance measure - Group 1

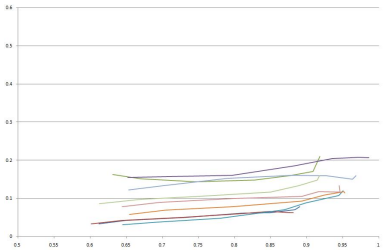

Figure A.7: Result of Cluster Analysis by means of Correlation Distance measure - Group 2

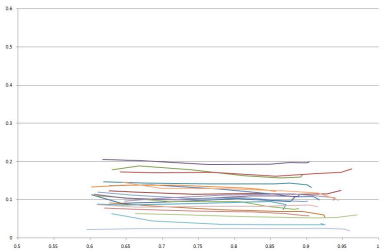

Figure A.8: Result of Cluster Analysis by means of Correlation Distance measure - Group 3

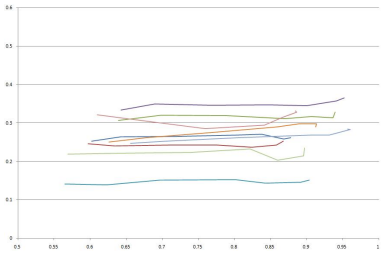

Figure A.9: Result of Cluster Analysis by means of Correlation Distance measure - Group 4

very similar, becomes possible to use a single element to represent the whole cluster.

This *representative item* can be easily built as *the mean element* of the cluster, that is the elements whose characteristics are the mean, weighted or not, of the characteristics of all the elements of the cluster.

To this ***centroid*** can be given a weight consisting in the number of elements of the cluster over the total number of elements of the sample, i.e.

a relative frequency.

This is exactly what we are interested in while applying the cluster analysis over our set of data for Demand and Wind Generation: resume all the characteristics of interest of our data, consisting of about 100 days values, in the lowest possible number of centroids.

A.5 How Many Clusters?

Another important point to be underlined is how to choose the correct number of clusters. The best way to evaluate the quality of the resulting clusters is to see the sum of the distances between elements of each cluster (also called ***intra-cluster distance***): the lower this sum, the better the cluster division.

Obviously, the higher the number of clusters we decide to build the lesser the number of elements which will belong to each cluster and, as a consequence, the more similar their characteristics, that is the lesser the distance between points in cluster.

On the other hand, the higher the number of clusters, the higher the number of representative items, the less effective the simplification on the system.

Thus, we have to take a trade off decision between the quality of the cluster division and the reduction in complexity of the problem. Unfortunately, this analysis cannot be performed *a priori*: we have to repeat the division in clusters for different times, each time increasing the number of cluster since we get an acceptable value in cluster's quality.

An example of this can be seen in figure A.10, where the sum of intra-cluster distances, by means of correlation measure, is plotted versus the num-

ber of cluster built. As we can see, already for 10 clusters the sum of distances is below 0.1, meaning that for the great part of the clusters the intra-cluster distance is below 0.01, i.e. correlation between points is higher than 0.99 which means a quasi-perfect allineation between points. Then, in this case, to use 10 clusters could be a good choice.

We have to underline that, especially for euclidean measure, the intra-

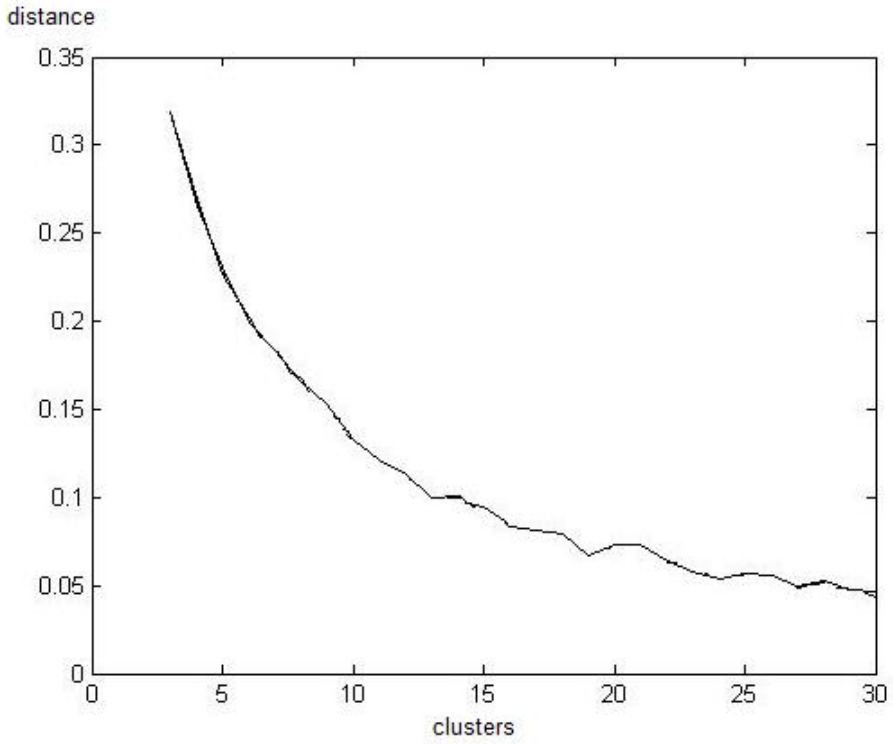

Figure A.10: Plot of sum of intra-cluster correlation distance versus number of clusters built

cluster distances, and as a consequence their sum, not always has an intuitive meaning. As a consequence, instead of setting a sort of "termination test" as for iterative cycles, is usually better to consider the sum of distance versus number of cluster curve.

This curve has a decreasing exponential tendency (as it's clearly showed in fig A.10), that is the reduction in sum of distance obtained by increasing the number of clusters is itself continuously decreasing by increasing the number of clusters. Thus, the best number of clusters is that one at which the addition of a new cluster does not cause a correspondingly significative improvement in the sum of distances.

By means of this criterion, the number of clusters chosen usually falls around 10 or 15, and never exceeds 20.

A.6 The MATLAB Function kmeans

Well-known algorithms exist to perform cluster analysis. Most of them are provided with common statistical packages for wide-spread numerical computing environments; an example is `kmeans` function for `MATLAB`.

This function is able to divide a sample in a number of clusters decided by the user, calculate the intra-cluster distance for each cluster, the sum of the intra-cluster distances and each cluster's centroid. Also, allows the user to choose between a set of 5 possible measures for distance, among which the most important are the two we have described in previous sections.

Other options allows the user to avoid local minima[2], improve convergence and improve the quality of the solution.

[2]Cluster construction is substantially an optimization problem, since its aim is to minimize the intra-cluster distance.

Appendix B

Development of a Technique for Testing Hypotheses about Correlation Coefficient Concerning Intervals of Values

In this sections we develop the technique we used to perform correlation tests. We based this work on the statistical theory as showed in [12].

Let us suppose to have 2 data series, X e Y, forming a Normal Bivariate population. Given the random variable r, *maximum likelihood estimator* for ρ (correlation coefficient for the 2 series), then the Fisher transformation for r is given by

$$U = \frac{1}{2} ln \frac{1+r}{1-r}. \tag{B.1}$$

For large n, number of elements forming the sample, $U \sim N(\mu, \sigma^2)$, where

$$\mu = \frac{1}{2} ln \frac{1+\rho}{1-\rho} \tag{B.2}$$

$$\sigma^2 = \frac{1}{n-3}; \tag{B.3}$$

here the only unknown is μ, while σ is known as we know n.

Suppose now we need to test if $\rho \in (\rho_1, \rho_2)$, knowing the estimated value $r = \tilde{r}$, from which follows $\tilde{u}$, by Fisher transformation (B.1). Let us consider the more general theory, as described in [12], which makes use of the likelihood function

$$L = \prod_{i=1}^{N} \frac{1}{\sqrt{2\pi \frac{1}{n-3}}} e^{-\frac{(\tilde{u}_i - \mu)^2}{2\frac{1}{n-3}}}. \tag{B.4}$$

Here N refers to the number of samples we handle, while n, as indicated above, is the number of elements forming the samples.

We call $\Omega = [-1, 1]$ the interval of all the possible values for ρ and $\omega = (\rho_1, \rho_2)$ the interval in which we want to test the presence of ρ. Then we can indicate with $L(\hat{\omega})$ the maximum, w.r. to the unknown parameter μ, of the function (B.4) in ω and with $L(\hat{\Omega})$ the maximum, again w.r. to μ, of the same function in Ω. We can thus define the ratio

$$\lambda = \frac{L(\hat{\omega})}{L(\hat{\Omega})}. \tag{B.5}$$

Usually we work with a single sample, that is $N = 1$. Then, we encounter the maximum of the likelihood function (B.4) in Ω when

$$\mu = \tilde{u}, \tag{B.6}$$

since this is the definition of maximum likelihood estimator; as a consequence

$$L(\hat{\Omega}) = \frac{1}{\sqrt{2\pi \frac{1}{n-3}}}. \tag{B.7}$$

Then, if we call $\hat{\mu}$ the value of μ that maximizes (B.4) in ω, we have

$$\lambda = e^{-\frac{n-3}{2}(\tilde{u} - \hat{\mu})^2}. \tag{B.8}$$

The theory, as exposed in [12], says that the closer λ is to 1, the more likely is the acceptance of the hypotheses. Then, we can build the following refusal condition

$$\lambda \in (0, A). \tag{B.9}$$

In order to calculate a value for A, we can consider λ as a function of $\tilde{u}$ and recognize that the function

$$\Lambda(\tilde{u}) = \sqrt{\frac{n-3}{2\pi}}\lambda(\tilde{u}) = \sqrt{\frac{n-3}{2\pi}}e^{-\frac{n-3}{2}(\tilde{u}-\hat{\mu})^2} \tag{B.10}$$

represents a *Normal probability density function* with mean $\hat{\mu}$ and variance $\sigma^2 = 1/(n-3)$.

Then, the condition (B.9) can be rewritten as

$$\Lambda \in (0, B), \tag{B.11}$$

where $B = \sqrt{\frac{n-3}{2\pi}}A$. Thus, a value for B, and then for A, can be easily calculated simply by solving for the interval (u_1, u_2) the equation

$$\int_{u_1}^{u_2} \Lambda(\tilde{u})d\tilde{u} = 1 - \alpha \tag{B.12}$$

where α is the ***level of confidence*** chosen.

We have to remark that this methodology comes out to be the classical *modus operandi* when our hypothesis is $\rho = \rho_0$, with the only difference that we have to consider the value $\hat{\mu}$, the one which maximizes the likelihood function (B.4) in the interval of interest for ρ, instead of $\mu_0 = \mu(\rho_0)$, calculated by equation (B.2).

As a final note, we have to underline that when $\tilde{r} \in (\rho_1, \rho_2)$, since $\omega \subset \Omega$ then the maximum of the likelihood function (B.4) in Ω, the global maximum, and in ω, a local maximum, coincide. As a consequence

$$\lambda = 1 \tag{B.13}$$

that means that the hypothesis $\rho \in \omega$ cannot be refused.

But we know from [12] and [13] that only the refusal of the hypothesis can be "certain" (with the level of confidence α); then, when $\tilde{r} \in \omega$ we

have to change the hypothesis to test from

$$\rho \in \omega \tag{B.14}$$

to

$$\rho \notin \omega. \tag{B.15}$$

Appendix C

Thermal Units Consumption Curves Definition

In this appendix, the definition of thermal units consumption curves is presented. A consumption curve is a function that indicates the efficiency of the transformation from the chemical energy in the fuel to the electric energy, that is the amount of fuel needed to produce the desired amount of electrical energy.

The efficiency has a very complex dependence on the level of the power output and the condition in which the unit is working (there is a great difference between stationarity and non stationarity) but is also influenced by all the external conditions that normally affect combustion processes. The combustion curve is thus only an approximation of what happens in reality, approximation which can take many formulations. In practice, the most used power curves are quadratic but with a quadratic term usually very small, such that also a linear approximation performs sufficiently well and allows the formulation of a linear programming model. Thus in s-MTSIM model linear consumption curves are considered.

C.1 Exact Linear Consumption Curves

In a MI linear model, fuel consumption for thermal unit u in hour t is modeled by means of the linear function

$$c(p)_{u,t} = B_{0u,t,\phi} \cdot \gamma_{u,t} + B_{1u,t,\phi} \cdot p_{u,t}, \tag{C.1}$$

indicating the amount of thermal energy $c(p)$, in [GJ], needed to produce the electric power output $p_{u,t}$. The value of parameters $B_{0u,t,\phi}$ and $B_{1u,t,\phi}$ depends on the technology used by thermal unit u and on the fuel ϕ burnt in the process. This function is represented by the consumption curve showed in figure C.1, where it is highlighted that when the status of the plant is *off*

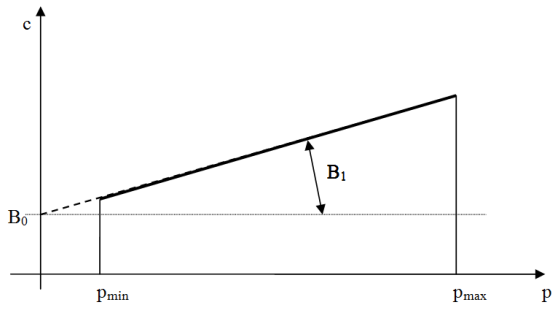

Figure C.1: Thermal Units Linear Consumption Curve

($\gamma_{u,t} = 0$ and $p_{u,t} = 0$) there is no fuel consumption.

For flexible thermal units, no lower bound on power output is usually prescribed (see constraints 9.4), then $B_{0f,t} = 0$ and the curve $c(p)_{f,t}$ takes the form represented in figure C.2.

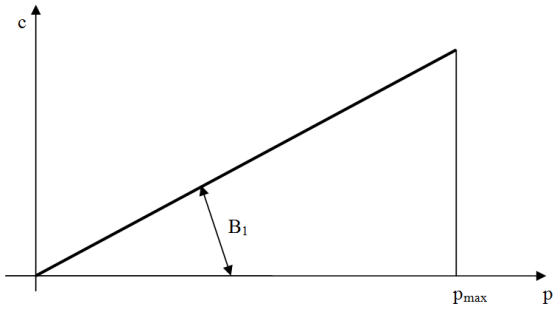

Figure C.2: Flexible Thermal Units Linear Consumption Curve

C.2 Modified Linear Consumption Curves

For non flexible thermal units g in a continuous formulation the minimum power output $\underline{p}_g^G$ is neglected (see section 9.2.1); then, for non flexible thermal units the correct linear consumption curve (red line in figure C.3) is substituted by a modified linear consumption curve (blue line in figure C.3),

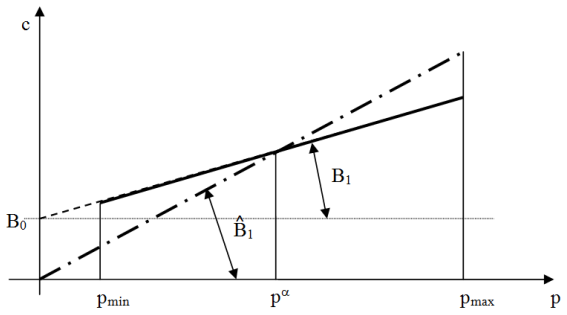

Figure C.3: Non Flexible Thermal Units Exact Linear Consumption Curve (red) vs. Modified Linear Consumption Curve (blue)

similar to the flexible units one.

The new linear term $\hat{B}_1$ is calculated as follows:

$$\hat{B}_{1g,t,\phi} = \alpha \frac{B_{0g,t,\phi}}{\overline{p}_g^G} + (1-\alpha)\frac{B_{0g,t,\phi}}{\underline{p}_g^G} + B_{1g,t,\phi}. \tag{C.2}$$

The weighting parameter α in equation (C.2) determines the point p^α of intersection of the exact curve with the modified one; since in the neighborhood of this point the difference between the two curves is negligible, it is important to set α such that p^α is as close as possible to the usual working point of the unit g. A typical value is $\alpha = 0.8$.

Appendix D

Calculation of Zonal Prices

In this appendix we will show how to calculate zonal prices for a power system model as formulated in chapter 9. For this purpose we will introduce and confront two models for the solution of a very simple version of UC Problem, formulated as follows:

- the system is divided into price zones $z \in \{1, \ldots, Z\}$,
- price zones are connected by interconnections $l \in \{1, \ldots, L\}$,
- generation devices $g \in \{1, \ldots, G\}$ are not differentiated by technology;

no time discretization is here considered since we do not want to develop a real model but only to obtain a mathematical formulation for the calculation of zonal prices.

The considered decision variables are thus:

- power generation p_g for each device g,
- power exchange between zones I_l on connection l,
- a slack variable for energy balance in zone z, S_z,

each with corresponding lower and upper bounds and lagrange multipliers:

$$\underline{p}_g \leq p_g \leq \overline{p}_g \quad \mu_g, \nu_g \tag{D.1}$$

$$\underline{I}_z \leq I_z \leq \overline{I}_z \quad \beta_z, \delta_z. \tag{D.2}$$

We furthermore consider:

- a variable cost c_g for device g,
- a price V for each MWh of unbalancing S_z in zone z,

and impose that the system must meet a zonal load K_z.

Since we want to solve the UC problem, the classical optimization problem (refer to [**?**] or to [14], for instance) looks for the minimum of the objective function

$$\phi = \sum_{g=1}^{G} c_g p_g + \sum_{z=1}^{Z} V \cdot S_z. \tag{D.3}$$

D.1 The "Global" Model

The first model we present is similar to the one developed in section **??**, since the following constraints are considered:

- a "global" balance over the whole system (from which the model name):

$$\sum_{g=1}^{G} p_g + \sum_{z=1}^{Z} S_z = \sum_{z=1}^{Z} K_z, \tag{D.4}$$

  for which we introduce the lagrange multiplier λ;

- the definition of the power exchange on each zonal interconnection l:

$$I_l = \sum_{z=1}^{Z} \sigma_{l,z} \left(p_{g \in G_z} + S_z - K_z \right) \tag{D.5}$$

  with the lagrange multiplier τ_l.

D.2 The "Zonal" Model

The second model is called zonal since it involves a zonal balance for each zone z instead of a global balance for the system:

$$\sum_{g \in G_z} p_g + S_z + \sum_{l \in L_z} (I_{l,IN} - I_{l,OUT}) = K_z, \tag{D.6}$$

with lagrange multipliers λ_z; the use of notation $I_{l,IN}$ and $I_{l,OUT}$ is a trick used to indicate the sign of the power exchange I_l on connection l from the point of view of zonal balance (respectively positive if represents an import of energy, negative if an export).

D.3 Zonal Prices

For the zonal model D.2, zonal prices are represented by lagrange multipliers λ_z of constraints D.6.

More difficult is the definition of zonal prices for the global model D.1: we have to consider its langrangian

$$\begin{aligned} \mathcal{G} \;=\; & \sum_{g=1}^{G} c_g p_g + \sum_{z=1}^{Z} V \cdot S_z + \lambda \left\{ \sum_{g=1}^{G} p_g + \sum_{z=1}^{Z} S_z - \sum_{z=1}^{Z} K_z \right\} + \\ & \sum_{l=1}^{L} \tau_l \left\{ I_l - \sum_{z=1}^{Z} \sigma_{l,z} \left(p_{g \in G_z} + S_z - K_z \right) \right\} + \\ & \sum_{g=1}^{G} \left\{ \mu_g \left(p_g - \underline{p}_g \right) - \nu_g \left(p_g - \overline{p}_g \right) \right\} + \sum_{l=1}^{L} \left\{ \beta_l \left(I_l - \underline{I}_l \right) - \delta_l \left(I_l - \overline{I}_l \right) \right\}. \end{aligned} \tag{D.7}$$

To solve the minimization problem we can calculate the derivatives of $\mathcal{G}$ w.r. to the decision variables and impose them to be equal to 0:

$$\begin{aligned}
\frac{\partial \mathcal{G}}{\partial p_g} &= c_g + \lambda - \sum_{l=1}^{L} \tau_l \sigma_{l,z} + (\mu_g - \nu_g) = 0; && \text{(D.8)} \\
\frac{\partial \mathcal{G}}{\partial S_z} &= V + \lambda - \sum_{l=1}^{L} \tau_l \sigma_{l,z} = 0; && \text{(D.9)} \\
\frac{\partial \mathcal{G}}{\partial I_l} &= \tau_l + \beta_l - \delta_l = 0. && \text{(D.10)}
\end{aligned}$$

Then, from D.10 $\tau_l = \delta_l - \beta_l$; thus, from D.8:

$$\lambda - \sum_{l=1}^{L} \tau_l \sigma_{l,z} = \lambda - \sum_{l=1}^{L} (\delta_l - \beta_l) \sigma_{l,z} = \nu_g - \mu_g - c_g. \qquad \text{(D.11)}$$

We can now perform the same operation with the zonal model, for which we can calculate the lagrangian:

$$\begin{aligned}
\mathcal{Z} &= \sum_{g=1}^{G} c_g p_g + \sum_{z=1}^{Z} V \cdot S_z + \\
&\sum_{z=1}^{Z} \lambda_z \left\{ \sum_{g \in G_z} p_g + S_z + \sum_{l \in L_z} (I_{l,IN} - I_{l,OUT}) - K_z \right\} + \qquad \text{(D.12)} \\
&\sum_{g=1}^{G} \left\{ \mu_g \left(p_g - \underline{p}_g \right) - \nu_g \left(p_g - \overline{p}_g \right) \right\} + \\
&\sum_{l=1}^{L} \left\{ \beta_l \left(I_l - \underline{I}_l \right) - \delta_l \left(I_l - \overline{I}_l \right) \right\},
\end{aligned}$$

and its partial derivatives w.r. to the decision variables::

$$\begin{aligned}
\frac{\partial \mathcal{G}}{\partial p_g} &= c_g + \lambda_z + \mu_g - \nu_g = 0; && \text{(D.13)} \\
\frac{\partial \mathcal{G}}{\partial S_z} &= V + \lambda_z = 0; && \text{(D.14)} \\
\frac{\partial \mathcal{G}}{\partial I_l} &= \pm \lambda_z + \beta_l - \delta_l = 0. && \text{(D.15)}
\end{aligned}$$

In particular, from D.13 we obtain $\lambda_z = \nu_g - \mu_g - c_g$ which, confronted to D.11 leads to obtain the following definition for zonal prices ψ_z:

$$\psi_z = \lambda_z = \lambda - \sum_{l=1}^{L} (\delta_l - \beta_l)\, \sigma_{l,z}. \tag{D.16}$$

Bibliography

[1] `www.talentfactory.dk/en/tour/wres/pwr.htm`. Technical report. (Danish Wind Industry Association).

[2] Ignacio Vizcaíno G. Sàenz de Miera, P. del Río González. Analysing the impact of renewable electricity support schemes on power prices: the case of wind electricity in spain. *Energy Policy*, 36:3345–3359, 2008.

[3] F. Chapman M. Milligan, A.H. Miller. Estimating the economic value of wind forecasting to utilities. Proceedings, Windpower '95 - Washington DC, March 27-30 1995.

[4] N. Vasilakos R. Green. Market behaviour with large amounts of intermittent generation. Technical report, Dept. of Economics - University of Birmingham.

[5] Design and operation of power systems with large amounts of wind power. State-of-the-art report, International Energy Agency, 2007.

[6] Integration of demand side management, distributed generation, renewable energy sources and energy storages. State-of-the-art report Vol. 1, International Energy Agency.

[7] H. Holttinen. Hourly wind power variations in the nordic countries. *Wind Energy*, 8:197–218, 2005.

[8] H. Ashraf-Ball J. Oswald, M. Raine. Will british weather provide reliable electricity? *Energy Policy*, 36:3212–3225, 2008.

[9] G. Sinden. Characteristics of the uk wind resource: Long-term patterns and relationship to electricity demand. *Energy Policy*, 35:112–127, 2007.

[10] `www.esios.ree.es`. Technical report. (Red Electica de España).

[11] El sistema eléctrico español '08. Technical note, Red Eléctrica de España, July 2009.

[12] F. A. Graybill A. M. Mood. *Introduction to the Theory of Statistics - 2nd ed.* MacGraw-Hill, 1963.

[13] F. J. Martin Pliego L. Ruiz-Maya Pérez. *Estadistica - II: Inferencia.* Editorial AC, 1995.

[14] W. Römish D. Dentcheva. *Optimal Power Generation under Uncertainty via Stochastic Programming*, volume Stochastic Programming Methods and Technical Applications of *Lecture Notes in Economics and Mathematical Systems*, pages 22–56. Springer-Verlag, 1998.

[15] N. P. Padhy. Unit commitment – a bibliographical survey. *IEEE Transactions on Power Systems*, 19(2):1196–1205, May 2004.

[16] R. Schultz C. C. Carø e. A two-stage stochastic program for unit commitment under uncertainty in a hydro-thermal power system. PREPRINT SC 98-11, KONRAD-ZUSE-ZENTRUM FUR INFORMATIONSTECHNIK, 1998.

[17] F. Aminifar A. Abiri-Jaromi M. Parvania, M. Fotuhi-Firuzabad. Reliability-constrained unit commitment using stochastic mixed integer programming. IEEE PMAPS, June 14th-17th 2010.

[18] P. Meibom C. Weber R. Barth, H. Brand. A stochastic unit-commitment model for the evaluation of the impacts of integration of large amounts of intermittent wind power. Stockholm, June 11th-15th 2006. IEEE PMAPS.

[19] F. D. Galiana J. F. Restrepo. Assessing the yearly impact of wind power through a new hybrid deterministic/stochastic unit commitment. *IEEE Transactions on Power Systems*, 26(1):401–410, Feb 2011.

[20] J. M. Arroyo M. Carrión. A computationally efficient mixed-integer linear formulation for the thermal unit commitment problem. *IEEE Transactions on Power Systems*, 21(3):1371–1378, Aug 2006.

[21] A. Zani. *An annual electricity market simulator: model description and application in a pan-European framework*. PhD thesis, Universitá degli Studi di Bergamo, 2011.

[22] J. de Joode G. Migliavacca A. Grassi A. Zani Ö. Ödzemir, K. C. Veum. The impact of large-scale renewable integration on europes energy corridors. IEEE Trondheim PowerTech, 2011. `ewh.ieee.org/conf/powertech/2011/`.

[23] M. Benini A. Grassi, A. Zani. A scenario analysis for an optimal pan-european cross-border network development. Zagreb, University of Zagreb, May 25th-27th 2011. International Conference on the European Energy Market (EEM11).

[24] A. Zani G. Migliavacca. A scenario analysis of the italian electricity market at 2020: emissions and compliance with the eu targets. Venice, June 17th-19th 2009. International Energy Workshop. `www.iccgov.org/iew2009/speakersdocs/presentazioni/19.06.2009/Parallel7/Alessandro%20ZANI.ppt.pdf`.

[25] `www.terna.it/default/Home/SISTEMA_ELETTRICO/mercato_elettrico/zone_di_mercato.aspx`. Technical report. (Terna - Italian TSO).

[26] S. W. Wallace P. Kall. *Stochastic Programming*. Wiley and Sons, 1st edition.

[27] www.terna.it/default/Home/SISTEMA_ELETTRICO/dispacciamento/Previsione_Prod_Eolica.aspx. Technical report. (Terna - Italian TSO).

[28] www.mercatoelettrico.org/En/MenuBiblioteca/documenti/20110705RelazioneAnnuale2010.pdf. Technical report, Gestore dei Mercati Energetici (Italian Energy Market Operator).

[29] www.terna.it/LinkClick.aspx?fileticket=M1GG5JSn7WY%3d&tabid=1265&mid=8582. Technical report. (Terna - Italian TSO).

[30] Cplex 12. Solver manual, GAMS. http://www.gams.com/dd/docs/solvers/cplex.pdf.

[31] Subbash Sharma. *Applied Multivariate Techniques*. John Wiley & Sons, 1996.